

# **Sponge Iron Process for Manned Space Exploration**

Ariadna Contract No. 18461/04/NL/MV

Technical officer: Dr. Tiziana Pipoli

- Final project report -

v + 71 pages  
June 2005

**Prepared by:**

Dr. Simon Fraser

Christian-Doppler Laboratory  
for Fuel Cell Systems  
Institute for Chemical Technology of Inorganic Materials  
Graz University of Technology  
Steyrergasse 21  
A-8010 Graz  
Tel. +43(0)316 873 8787  
Fax +43(0)316 873 8782  
simon.fraser@TUGraz.at

**Head of the Laboratory:**

Dr. Viktor Hacker

Christian-Doppler Laboratory  
for Fuel Cell Systems  
Institute for Chemical Technology of Inorganic Materials  
Graz University of Technology  
Steyrergasse 21  
A-8010 Graz  
Tel. +43(0)316 873 8780  
Fax +43(0)316 873 8782  
viktor.hacker@TUGraz.at

**Head of the Institute:**

Prof. Jürgen O. Besenhard

Institute for Chemical Technology of Inorganic Materials  
Graz University of Technology  
Stremayrgasse 16/III  
A-8010 Graz  
Tel. +43(0)316 873 8260  
Fax +43(0)316 873 8272  
besenhard@TUGraz.at



---

## Table of contents

---

<b>EXECUTIVE SUMMARY .....</b>	<b>1</b>
<b>1 INTRODUCTION.....</b>	<b>3</b>
1.1 Objectives of this study .....	4
1.2 Overview of the investigations .....	4
1.3 Applying mathematical modelling as tool for determining RESC system performance.....	5
<b>2 FUNDAMENTAL PRINCIPLES OF SPONGE IRON REACTOR/RESC OPERATION 6</b>	<b>6</b>
2.1 Principle of the sponge iron reaction.....	6
2.2 Principle of the reformer sponge iron cycle (RESC) .....	8
2.3 SIR operation with gases containing impurities such as sulphur .....	9
<b>3 POTENTIAL APPLICATIONS OF THE STEAM IRON PROCESS IN ISRU APPLICATIONS ON MOON AND MARS.....</b>	<b>10</b>
3.1 ISRU in the case of the Moon .....	10
3.1.1 Surface resources on Moon.....	10
3.1.2 Oxygen production on the Lunar surface.....	12
3.2 ISRU on Mars .....	13
3.2.1 Atmospheric resources on Mars .....	13
3.2.2 Surface and subsurface resources on Mars .....	13
3.2.3 Fuel and oxygen production on the surface of Mars.....	15
3.3 On the utilisation of Lunar and Martian surface materials as contact mass for the sponge iron cycle.....	16
3.4 Possibilities of SIR/RESC operation in missions to Moon and Mars.....	18
<b>4 MATHEMATICAL MODELLING OF THE RESC PLANT .....</b>	<b>20</b>
4.1 Aim of the mathematical model.....	20
4.2 Mathematical modelling of the hydrocarbon reformer.....	20
4.2.1 Introduction to mathematical modelling of the hydrocarbon reformer.....	20
4.2.2 Governing equations of the reformer model .....	20
4.2.3 Implementation of the hydrocarbon reformer model.....	21
4.2.4 Example calculation of the hydrocarbon reformer model.....	22
4.3 Mathematical modelling of the Sponge Iron Reactor (SIR).....	23
4.3.1 Introduction to mathematical modelling of the sponge iron reaction.....	23
4.3.2 Governing equations of the sponge iron reactor model .....	23
4.3.3 Implementation of the sponge iron reactor model.....	25
4.4 Mathematical modelling of the complete RESC plant.....	25
4.4.1 Auxiliary devices required in a RESC plant .....	25

4.4.2	Overview of the RESC process in reduction mode.....	26
4.4.3	Overview of the RESC process in oxidation mode .....	27
4.4.4	Input species considered with the RESC simulation.....	27
4.4.5	Example calculation performed with the RESC model .....	29
<b>5</b>	<b>APPLYING THE RESC FOR HYDROGEN PRODUCTION FROM A READY HYDROCARBON INPUT SPECIES .....</b>	<b>32</b>
5.1	Mass balance of the conversion process.....	32
5.1.1	RESC hydrogen production capability .....	33
5.1.2	Additional hydrocarbon fuel required for heating purposes .....	33
5.1.3	Overall molar flux supplied to the SIR.....	34
5.1.4	Fuel utilisation of the SIR as a function of operating condition .....	35
5.1.5	Mass balance of the input species considered .....	35
5.2	Thermal energy balance of the conversion process .....	38
5.3	Hydrocarbon to hydrogen conversion efficiency .....	39
5.3.1	Variation of the conversion efficiency with recycle rate and temperature .....	39
5.3.2	Conversion efficiency for the investigated RESC input species .....	40
5.4	Evaluation of RESC system performance as a function of input gas.....	42
5.5	Investigations of the combined RESC/fuel cell system.....	45
5.5.1	RESC/fuel cell system with intermediate storage .....	45
5.5.2	Direct combination of RESC and high-temperature SOFC.....	47
5.5.3	Thermodynamic investigation of the direct RESC/SOFC combination .....	49
5.6	Compilation of key results derived with the RESC system simulations .....	53
<b>6</b>	<b>APPLYING THE SIR FOR OXYGEN EXTRACTION FROM LUNAR REGOLITH .....</b>	<b>54</b>
<b>7</b>	<b>HYDROGEN PRODUCTION WITH CARBON MONOXIDE AS SIR REDUCING AGENT.....</b>	<b>57</b>
<b>8</b>	<b>APPLYING THE SIR FOR ENERGY STORAGE PURPOSES .....</b>	<b>59</b>
	<b>LIST OF ABBREVIATIONS.....</b>	<b>61</b>
	<b>LIST OF FIGURES.....</b>	<b>62</b>
	<b>LIST OF TABLES .....</b>	<b>64</b>
	<b>REFERENCES.....</b>	<b>66</b>
	<b>APPENDIX A: CHEMICAL COMPOSITION OF LUNAR SOILS .....</b>	<b>69</b>
	<b>APPENDIX B: EVALUATION SCORE TABLES.....</b>	<b>70</b>

## Executive Summary

REDOX cycling of an iron-rich contact mass has been investigated and applied with terrestrial hydrogen production from hydrocarbon and biomass sources. The governing principle utilised with this process is to discontinuously supply reducing gases (i.e. a synthesis gas with a high content of hydrogen and/or carbon monoxide) and steam into a reactor filled with iron pellets (the so-called contact mass). The contact mass is thus either reduced or oxidised, depending on the supply with synthesis gas or steam. By applying either a single reduction step or repeated REDOX cycles, the fundamental sponge iron reaction can thus be utilised with a wide range of different applications.

The fundamental sponge iron reaction principle could also be utilised with a number of different applications in space missions. Surface regolith with a high iron content – being widely available on Moon and Mars - provides a feasible resource for the process contact mass, and enables a number of different approaches and concepts for utilisation. The possibilities and limitations of utilising the sponge iron reaction with different applications in missions to the surface of Moon and Mars have been investigated within this research project.

Four different applications of the sponge iron reaction have been considered within this initial study. The applications were investigated with a detailed thermodynamic model, comprising of components models of the sponge iron reactor (SIR), the hydrocarbon reformer, and the different auxiliary devices required to operate the process. Results of the thermodynamic simulations applied with each of the investigated applications are presented and discussed within this final study report.

The first application investigated within this project is the production of pure fuel cell grade hydrogen from different hydrocarbon species. The reformer sponge iron cycle (RESC), an innovative process combining a sponge iron reactor with a hydrocarbon reformer and a partial off-gas feedback loop, was investigated as means of providing an on-site hydrogen production capacity from a feedstock of hydrocarbons produced with ISRU technology and/or supplied from Earth. Based on thermodynamic considerations, conversion efficiencies in the order of 75-80% (LHV product hydrogen versus LHV input hydrocarbon species) were derived with methane, LPGs (propane, butane), and liquid hydrocarbons (heptane, octane) as RESC input species. Conversion efficiencies for alcohols (methanol, ethanol) were slightly smaller, being in the order of 67-75%. The hydrocarbon to hydrogen conversion process is generally exothermic in the reduction cycle (reduction of iron contact mass, oxidation of gas phase) with all investigated input species, whereas the oxidation cycle (oxidation of iron contact mass, reduction of gas phase) is generally endothermic. The overall thermal energy balance is thus positive for all fuels except of methanol. An additional heat source (e.g. hydrocarbon burner unit, heat coming from a nuclear reactor) therefore has to be considered with most of the hydrocarbon input species, even with the simplified thermodynamic calculation utilised for system analysis.

Calculated overall fuel to electric conversion efficiencies of the combined RESC/fuel cell system are in the order of 38-44%, depending on the type of input species and the process heat supply. Significantly higher conversion efficiencies are derived for a direct combination design, where the RESC is operated with a high-temperature solid oxide fuel cell (SOFC) within the same thermal enclosure. Applying fuel cell off-gas recycling with the RESC oxidation cycle, hydrocarbon to electric conversion efficiencies in excess of 45% are derived with the thermodynamic analysis of this direct combination design approach.

The second investigated application is the extraction of oxygen from lunar regolith. This extraction process is based on a single reduction process with hydrogen, producing a steam/hydrogen reactor output gas. SIR reduction cycle product water would have to be condensed and electrolysed to produce oxygen and hydrogen. Thermodynamic modelling of the process was applied to investigate the utilisation of hydrogen within the reactor, and to derive a thermal energy balance of the reduction process. The oxygen extraction process was derived as being mildly exothermic with the utilised thermodynamic system analysis. A further-going analysis would have to be applied with a thorough investigation of process, though. Thermodynamic data of the extraction process alone does not provide the level of insight required with an accurate prediction of the overall extraction system performance. This issue would have to be specifically addressed with a detailed modelling effort.

Two theoretical applications of the sponge iron process were also investigated within this study: hydrogen production with carbon monoxide as SIR reducing agent, and storage of hydrogen by means of a REDOX reaction of a contact mass. The former is based on feeding (pure) carbon monoxide into the reactor and utilising the input gas for contact mass reduction. Steam could then be fed into the reactor in a second step, re-oxidising the contact mass and thus converting a fraction of input steam into pure hydrogen. Thermodynamic limitations of the conversion process in reduction mode prevent a full utilisation of the carbon monoxide input gas. Some 35% of the input carbon monoxide cannot be utilised with the desired reduction process at a temperature of 800°C and must be utilised e.g. for heating purposes. Low rates of utilisation are therefore an issue that strongly limits the range of applicability.

Storage of hydrogen by reducing an iron-rich contact mass and re-oxidising it on demand with steam at elevated temperatures is a second theoretical application. Hydrogen storage capacities in the order of 4.8 wt% were determined for a full oxidation into Magnetite. Correspondingly smaller values have to be considered with a contact mass containing minerals that do not contribute to the REDOX reactions. This would be the case with an application based on locally available regolith on Moon or Mars, where the surface material normally contains less than 20 wt% of iron. Maximum hydrogen storage capacities would thus be in the order of 1 wt% for average regolith material with a full cycling of the contact mass iron content.

## 1 Introduction

Reduction of oxidised iron species is a well-established technology utilised in iron metal production. The basic principle applied in this process is to reduce the iron oxides with reducing gases – primarily synthesis gases with a high content of carbon monoxide and/or hydrogen - at elevated temperatures in a furnace. Thus, iron metal production is governed by a REDOX reaction, involving the oxidation of a gaseous species and the simultaneous reduction of the solid iron ore. If the reaction proceeds into the opposite direction, the iron metal is oxidised back into different stages of oxidation. This process is referred to as rusting if it occurs at ambient atmosphere, and completes a full cycle from iron oxide into iron metal and back into the oxidised state.

Already at the beginning of the last century, this well-known REDOX reaction was not only utilised for iron metal production, but also for hydrogen production. REDOX cycling of iron was thus utilised as means of converting steam into hydrogen. This hydrogen production process was utilised to produce large quantities of hydrogen gas at the beginning of the last century, required primarily for applications in the field of aerial navigation [1]. Renewed interest in this so-called sponge iron reaction was recently reported with different research activities, proposing the use of the process for converting synthesis gas produced from solid biomass into fuel cell grade hydrogen [2,3].

The low conversion efficiencies achieved with the basic sponge iron reaction process led to the development of the Reformer Sponge Iron Cycle (RESC) [4]. The RESC is based on the combined operation a sponge iron reactor with a hydrocarbon reformer unit and a special off-gas management system. Combining the simple, but limited operational capabilities of the sponge iron reaction with the possibilities of a hydrocarbon reformer based system provides an innovative means of producing hydrogen. The process essentially enables the conversion of hydrocarbons, alcohols, or virtually any kind of solid, liquid, or gaseous input species that can be converted into a hydrogen- and/or carbon monoxide-rich gas, into pure hydrogen. For the case of terrestrial applications, fossil sources (e.g. natural gas, liquid petroleum gas, Diesel) as well as regenerative sources (e.g. biogas, bio-methanol, bio-ethanol) could thus be utilised as input species with the RESC hydrogen production process.

In space applications, the RESC is particularly interesting in combination with in-situ resource utilisation (ISRU) technology. Thus, e.g. hydrocarbon fuels could be converted into fuel cell grade hydrogen directly on the surface of Mars. Regolith with high iron content could serve as contact mass (i.e. the solid volume involved in the REDOX reaction) with a system based on a repeated REDOX cycling, or a single reduction step, respectively.

Initial investigations that have been conducted in the search for promising applications of the sponge iron cycle as well as the RESC system with space missions to Moon and Mars are summarised in this final project report.

## 1.1 Objectives of this study

The RESC, as well as the fundamental steam-iron process, offer interesting possibilities not only in terrestrial, but also in space applications. This is particularly true with missions to the surface of Moon and Mars, where the surface regolith contains significant quantities of oxygen bound in minerals with a high iron(oxide) content. Surface regolith could thus be utilised as contact mass in a steam-iron process, and not only serve as a source of oxygen, but also as a means of producing, cleaning, and storing hydrogen gas e.g. for fuel cell applications.

The following aspects have been investigated within this initial study on sponge iron reaction utilisation and performance analysis in space applications on Moon and Mars:

- Assessment of the feasibility of the reformer sponge iron process for applications on Moon and Mars; primarily fuel production with Mars ( $H_2$ , CO) and oxygen extraction with the Moon
- Investigation of the energy balance of the process (thermal and chemical energy balance)
- Investigations of the overall efficiency of the process (fuel conversion efficiency)
- Investigation of the possibilities of operating the process with different input species, considering the role of  $CO_2$  from the atmosphere of Mars as well as of hydrocarbons brought from Earth and of (ISRU-produced) methane
- Optimisation of the process for the environmental conditions encountered on the surface of Moon and Mars (e.g. operating temperature)
- Assessment of the operation of the process with gases containing impurities such as sulphur
- Investigation of the overall energy balance of the process when operated with a fuel cell (PEMFC and SOFC)

## 1.2 Overview of the investigations

In order to enable a thorough analysis of the possibilities and limitations of operating the sponge iron process - or the RESC, respectively - in missions on Moon and Mars, a special emphasis was put on investigating the following issues:

- Investigation of surface resources and in-situ resource utilisation (ISRU) concepts developed for Moon and Mars

- Generation of a summary of potential applications of the sponge iron process with missions to the surface of Moon and Mars
- Development of a complete mathematical model of the RESC process including a detailed analysis of the different system components involved (e.g. sponge iron reactor, hydrocarbon reformer unit, gas management system)
- Full analysis of the possibilities and the limitations of operating the sponge iron process on the surface of Moon and Mars by applying system simulations

Mathematical modelling is a flexible and powerful tool commonly applied to provide fundamental figures about the performance of a system operated under certain pre-defined conditions. Performance figures derived with the mathematical models can be referred to as “theoretical limits” that cannot be exhibited in practise, following the fundamental thermodynamic considerations applied with the development of the models. If results achieved with initial system modelling are promising, a deeper analysis of the system suggests itself. This deeper analysis could be based on a more detailed theoretical system analysis, where the various assumptions and simplifications applied with the initial model are re-considered and refined. The second option would be to proceed with an experimental investigation of system elements operated and analysed under realistic operating conditions.

### **1.3 Applying mathematical modelling as tool for determining RESC system performance**

The RESC essentially has three key parameters that determine design, operation, and efficiency of the process: input species, RESC process temperature, and SIR offgas recycle rate. Operating the RESC process with different hydrocarbon input species is not only an interesting aspect with respect to the ability to adapt the process to specific fuel options, but also with respect to key design criteria. Designing a RESC plant operating with higher hydrocarbons (e.g. pure liquid hydrocarbons such as heptane, or a mixture of different hydrocarbons such as Diesel, for instance) requires a different plant layout including hydrocarbon evaporators and a pre-reformer unit that are not required with the basic RESC design that is operated directly with methane (or natural gas, respectively) as fuel. SIR process temperatures and recycle rates have to be optimised for a specific application in order to derive a plant layout that is efficient, but nevertheless small enough to be installed into a compact package. Both parameters are linked by the fact, that the lean gas stream is burned in the lean gas burner unit. Thus, the input of thermal energy into the RESC process is closely linked to the recycle gas rate, unless an additional heat source is installed into the system.

The contact mass is the fourth major parameter that determines operational characteristics and capability of the system. Applying a contact mass that is able to reduce and/or to oxidise large quantities of input gas at high rates leads to a high performance system capable of providing high hydrogen production rates.

A schematic overview of the governing operational parameters of the RESC system is shown in Figure 1.

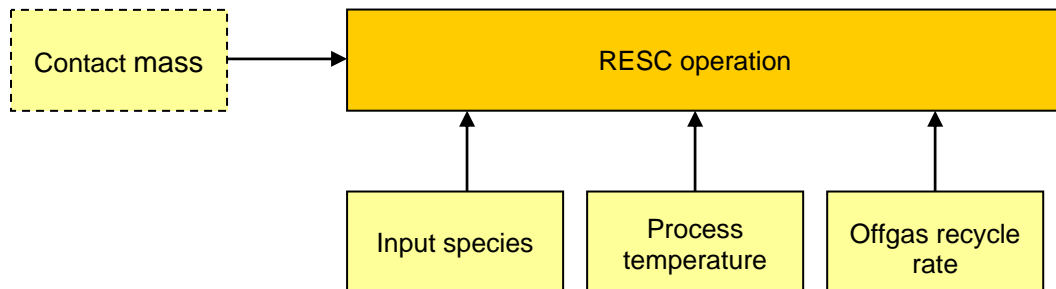


**Figure 1** Governing parameters in RESC operation

Utilising the instrument of mathematical modelling, the dependence between operational parameters and RESC system performance can be thoroughly investigated. This provides key information in the subsequent process of performance analysis and evaluation.

## 2 Fundamental principles of sponge iron reactor/RESC operation

### 2.1 Principle of the sponge iron reaction

The fundamental process investigated with different applications in the field of hydrogen and/or oxygen production is the so-called steam iron process. This process is based on discontinuously supplying a sponge iron reactor (SIR) with reducing gases (containing hydrogen and carbon monoxide) and steam. The former species reduces the contact mass from magnetite ( $\text{Fe}_3\text{O}_4$ ) and wuestite ( $\text{FeO}$ ) into iron metal ( $\text{Fe}$ ) if the gases contain sufficient quantities of hydrogen and carbon monoxide. Laboratory investigations performed in a previous research project at Graz University of Technology revealed, that traces of hydrocarbons (e.g. methane), that are fed into the SIR, do not contribute a considerable share to the overall reduction process of iron oxides. Thus, a high content of hydrogen and carbon monoxide has to be envisaged with the SIR input gases. Once all of the magnetite and wuestite inside the reactor has been reduced, the supply with reducing gases is stopped, and hot steam is fed into the reactor. The iron pellets are thus oxidised back into the wuestite and/or magnetite stages, converting a fraction of the steam supplied into pure hydrogen. Alternatively, carbon dioxide could also be used as input gas in the oxidation process of iron metal. Solid carbon formation phenomena could be a limiting aspect in SIR operation with carbon dioxide input gas, though.

The basic reactions occurring within the standard SIR are outlined below. Two main reactions are identified with operating conditions commonly faced in the SIR: firstly, a conversion step between iron metal ( $\text{Fe}$ ) and wuestite ( $\text{FeO}$ ), and secondly a conversion step between wuestite ( $\text{FeO}$ ) and magnetite ( $\text{Fe}_3\text{O}_4$ ). The standard SIR process is based on REDOX cycling of an iron-based contact mass. Thermodynamic and kinetic performance of

other metals commonly found in regolith on the surface of Moon and Mars would have to be determined in laboratory investigations as well as thermodynamic calculations. For the case of these initial investigations, the active contact mass is assumed to consist of iron(oxide); the remaining constituents are assumed to be inactive and therefore do not contribute to the REDOX reactions. Only a limited number of minerals have been investigated with respect to their influence on contact mass performance. The effect of adding different quantities of  $\text{SiO}_2$ ,  $\text{CaO}$ , and  $\text{Al}_2\text{O}_3$  to the iron contact mass has been recently investigated in the CD-Laboratory. First results of these investigations were submitted to the International Journal of Hydrogen Energy [5].

The iron/wuestite equilibrium can be written as:



The magnetite/wuestite equilibrium can be written as:



Two operating conditions are defined for the SIR: *reduction mode* and *oxidation mode*. In *reduction mode*, the contact mass is reduced from magnetite to wuestite and on to iron metal (if the gas contains sufficient quantities of hydrogen and/or carbon monoxide). The solid contact mass is thus reduced, whereas the gas is oxidised with the oxygen removed from the contact mass. The opposite reaction occurs in *oxidation mode*. Here, the contact mass is re-oxidised, drawing oxygen out of the gas phase. The gases are therefore reduced, which produces pure hydrogen in the case of a feed of steam. The SIR operating principle is shown in Figure 2.

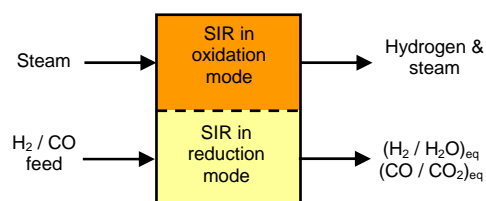


**Figure 2** Simplified schematic of the SIR

Hydrogen produced by the SIR offers a very high purity and does not contain significant quantities of carbonaceous species due to the fact that steam is the only input species in the oxidation cycle. This is of special importance with respect to carbon monoxide catalyst poisoning effects reported for low-temperature polymer electrolyte membrane fuel cells [6,7]. SIR offgas in oxidation mode can thus be directly stored e.g. in a high pressure storage vessel after removing the steam. No extensive measures for gas clean-up are required if the process is operated appropriately (e.g. no carbon formation).

## 2.2 Principle of the reformer sponge iron cycle (RESC)

The reformer sponge iron cycle (RESC) is based on the SIR, but introduces an additional hydrocarbon reformer as well as a partial offgas recycling system. This setup provides considerable advantages compared to the standard SIR system, primarily with respect to the fuel to hydrogen conversion efficiency and to the operational capabilities. The recycling loop proved to be particularly beneficial due to the fact that offgas – that would be lost with the standard SIR process – can thus be utilised as source of heat for the endothermic reforming reaction. Thus, the flux of energy leaving the SIR is not lost for the conversion process, but is rather applied to produce additional quantities of hydrogen and/or carbon monoxide in the reformer unit.

Figure 3 shows a strongly simplified schematic of the RESC plant layout. Operating the RESC in *oxidation mode* is a straight-forward process converting steam into a mixture of steam and hydrogen, as outlined above. Operation in *reduction mode* is governed by recycling a fraction of SIR offgas and adding the fresh hydrocarbon fuel into this stream of partially oxidised gases. The advantage of this partial recycling of offgas is twofold: firstly, SIR offgas contains considerable quantities of hydrogen and carbon monoxide. A fraction of this gas can be utilised in the reduction process of iron pellets by re-feeding the gas back into the SIR. The second key advantage is that no additional steam has to be generated for the reforming reaction. The hot SIR offgas contains sufficient quantities of steam and carbon dioxide to enable a full conversion of the hydrocarbon fuel with a wide range of recycling rates. The fraction of SIR offgas that is not recycled is combusted with ambient air (or pure oxygen) in a burner unit. Heat produced by the combustion is subsequently used to evaporate and heat the input hydrocarbon species to process temperature.

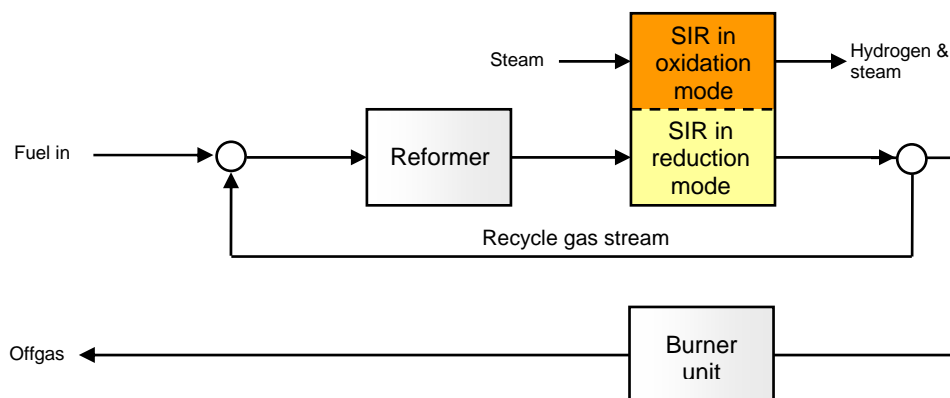


**Figure 3** Simplified schematic of the RESC

A laboratory-scale RESC system has been developed and successfully operated at Graz University of Technology. The system consists of the sponge iron reactor (the blue cylindrical device shown on the left hand side of Figure 4) that can be supplied with gas

coming either from the gas mixing station or a reformer unit where gaseous (e.g. methane) as well as liquid hydrocarbons (e.g. heptane) can be utilised with a small pre-reformer and a main reformer unit. Operational data generated with the RESC test rig enables a fundamental proof-of-concept, and is also applied for model validation.



**Figure 4** RESC test rig installed at Graz University of Technology

### 2.3 SIR operation with gases containing impurities such as sulphur

Operation of the SIR with gases containing impurities commonly included with synthesis gas produced from fossil or biomass sources has been previously investigated with the SIR test rig. Laboratory investigations revealed, that the SIR can be successfully operated with input gases containing traces of hydrogen sulfide ( $H_2S$ ) and hydrogen chloride ( $HCl$ ) [8]. Lean gas leaving the reactor in reduction mode offered similar volume fractions of the respective species, whereas the hydrogen produced in the oxidation cycle was extremely pure. After condensing the water vapour out of the SIR offgas in oxidation mode, the hydrogen chloride content was in the order of 3-4 ppm, the content of hydrogen sulfide was even lower, being less than one ppm. Thus, the impurities did not affect the process, but were rather removed out of the system with the lean gas. Long-term stability of the contact mass operated with these impurities is to be determined, though.

A compressed overview of gas compositions in reduction and oxidation mode, applied in the aforementioned investigations with gases having the respective impurities, is presented in Table 1.

**Table 1** Composition of inlet gas, lean gas and product hydrogen (in percent per volume if not stated otherwise) after conversion in the SIR

	N <sub>2</sub>	H <sub>2</sub>	H <sub>2</sub> O	CO	CO <sub>2</sub>	HCl	H <sub>2</sub> S
Input gas	31-32	20-23	18-20	12-14	12-13	0-0,02	0-0,05
Lean gas	31-32	12-14	29-31	6-7	18-20	0-0,015	0-0,05
Produced hydrogen <sup>1)</sup>	n/a	> 99	n/a	30 ppm	100 ppm	3-4 ppm	< 1ppm

<sup>1)</sup> gas after vapour condensation

### 3 Potential applications of the steam iron process in ISRU applications on Moon and Mars

Moon and Mars are commonly referred to as two of the most promising cases for applications of ISRU technology. The following chapter will provide a brief overview about the different concepts that are currently being investigated with the respective applications. Possibilities and limitations of introducing the RESC as innovative means of combining the fuel cell-grade hydrogen production capability of the steam iron process with a hydrocarbon reformer unit is discussed with a selection of potential input species options.

#### 3.1 ISRU in the case of the Moon

The Moon does not have any atmospheric resources that could be extracted. The extremely low atmospheric pressure ( $3 \times 10^{-15}$  bar at night [9]) is prohibitive for utilisation, leaving surface and subsurface minerals as only source for ISRU. Surface regolith is highly oxidised, providing a readily-available source of oxygen. The surface layer is also rich in metals (e.g. Fe, Ti, Al) which is of special interest with the investigated operation of a SIR/RESC unit on the lunar surface.

##### 3.1.1 Surface resources on Moon

A compressed overview of surface compositions measured with different samples collected with the American Apollo missions and Russian Lunar missions is presented in Table 27 in Appendix A on page 69. Large fractions of the surface probes analysed are oxygen (some 40% bound in molecular silicates and metal oxides [10]). Mining this oxygen from readily available surface resources suggests itself. Thus, the large quantities of oxygen needed for life support systems and propellant oxidisers could be produced directly on the Lunar surface, rather than transporting a full supply from Earth.

More than 20 different processes have been proposed for oxygen production from lunar surface materials. One of the most promising processes is to utilise the mineral ilmenite (FeTiO<sub>3</sub>) - which is widely available - for oxygen production according to equation E3 [11].

A two-step oxygen production process is commonly applied. The lunar material is heated under a reducing atmosphere - such as hydrogen - in the first step. This produces steam as gaseous reaction product. Oxygen is separated in an electrolysis unit and can be subsequently stored in a cryogenic storage vessel. Hydrogen can be re-fed back into the system, and is thus not lost for the oxygen production process.



NASA has conducted investigations with different lunar soils representing the compositions measured with the Apollo mission samples. Characterisations at 1050°C showed, that there is a strong link between the gravimetric oxygen yield and the amount of iron oxide in the sample [11]. The measured correlation between oxygen yield and FeO content is presented in Figure 5 for 14 soils and the volcanic glass 74220 [11].

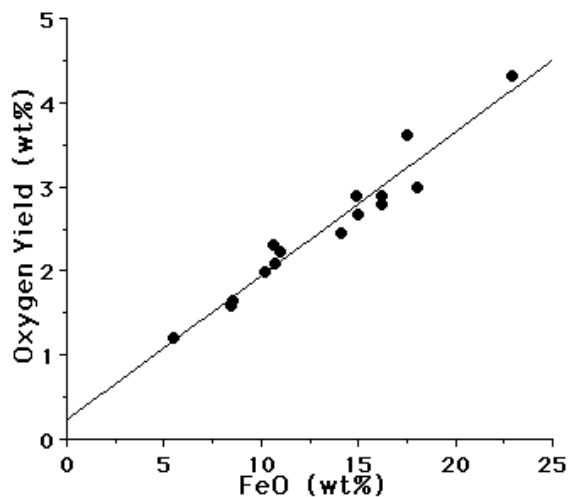


**Figure 5** Oxygen yield (mass of oxygen per mass of starting material) for 14 lunar soils and one lunar volcanic glass reacted at 1050°C [11]

Concentrations of FeO on the lunar surface layer show strong regional variations. The Apollo landing sites showed FeO concentrations in the range of 5-17 wt%. Recent investigations conducted with the Clementine spacecraft [12] provide a good overview about the regional concentrations of FeO.

Regional distribution of iron oxide on the lunar surface is shown in Figure 6.

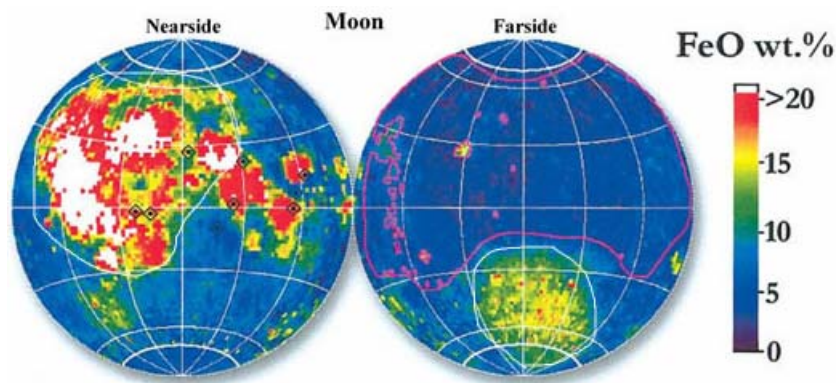


**Figure 6** Regional distribution of iron oxide concentrations on the Moon [13]

### 3.1.2 Oxygen production on the lunar surface

A large fraction of the overall spacecraft propulsion system mass is consumed by oxygen. Thus, some 85% of the return flight propellant mass (i.e. the flight from the Moon back to Earth) could be saved with a hydrogen/oxygen-fuelled spacecraft, if the oxygen would not have to be taken from Earth, but could rather be produced directly on the Lunar surface [14]. Thus, the Earth launch mass would be drastically reduced, which is one of the key issues in bringing down mission costs.

Figure 7 gives an artist's impression of a lunar oxygen production plant, where remotely-driven vehicles are utilised to transport lunar soil to the production facility. Oxygen produced by the plant is liquefied and stored in cryogenic storage vessels. The plant is built around a hydrogen reduction process with a three-stage fluidised bed reactor and a 40-60 kW nuclear power supply. This plant would be able to produce sufficient quantities of oxygen to return a crew of four from the Moon twice a year. The stored liquid oxygen would have to be pumped into the crew return vehicle prior to lift-off by means of oxygen "tankers" similar in design to the tele-operated front-end loaders that are utilised for mining regolith and disposing the off-products [15].



**Figure 7** Lunar oxygen production plant (NASA/JSC image #S93-45590)

## 3.2 ISRU on Mars

### 3.2.1 Atmospheric resources on Mars

The atmosphere on Mars is thin (variable from 4.0 – 8.7 mbars [16]), but nevertheless contains considerable quantities of gases that could play a key role in producing propellants and/or consumables directly on the surface of Mars. Particularly the high content of carbon dioxide is interesting with respect to producing oxygen and carbon monoxide. Carbon monoxide could either be utilised directly as propellant for a CO/O<sub>2</sub> propulsion system, or could be utilised for power generation in a high-temperature fuel cell. Utilising the sponge iron reaction, carbon monoxide could also be utilised as reducing agent for the contact mass. This would provide a means of producing additional quantities of hydrogen by utilising steam for re-oxidation of the pellets.

Composition of the Martian atmosphere is presented in Table 2. Seasonal variations in absolute and relative pressures of the individual species have to be considered with a detailed analysis of atmospheric gas composition.

**Table 2** Composition of the Martian atmosphere [16]

Carbon dioxide	CO <sub>2</sub>	95.32%
Nitrogen	N <sub>2</sub>	2.7%
Argon	Ar	1.6%
Oxygen	O <sub>2</sub>	0.13%
Carbon monoxide	CO	0.08%
Water	H <sub>2</sub> O	210 ppm
Nitrogen Oxide	NO	100 ppm
Neon	Ne	2.5 ppm
Hydrogen-Deuterium-Oxygen	HDO	0.85 ppm
Krypton	Kr	0.3 ppm
Xenon	Xe	0.08 ppm

### 3.2.2 Surface and subsurface resources on Mars

The Martian surface has been investigated at three different locations by the two Viking Lander units and the Mars Pathfinder (MPF) Lander / Sojourner. The twin NASA Mars exploration rovers (MER) are currently investigating surface samples on a regional basis. Data from the current MER missions is still very limited, this report will therefore present results from the Viking and MPF missions, only.

The elemental composition of the Martian surface is presented in Table 3. Values presented from VL1 are derived from measurements with the Viking X-Ray Fluorescence Experiment [17]. The data is compared with two measurements performed with the MPF Alpha Particle X-Ray Spectrometer (APXS) applied to analyse the rock sample “Barnacle Bill”, denoted MPF A3 in Table 3, and the soil sample A5 extracted near the rock “Yogi” [18].

**Table 3** Elemental composition of samples at the Viking 1 Lander and MPF Lander sites (wt%) [17,18]

	VL1	MPF A3 <sup>1</sup>	MPF A5 <sup>1</sup>
O	n/a	45.0	43.2
Na	n/a	3.1	2.6
Mg	5.0	1.9	5.2
Al	3.0	6.6	5.4
Si	20.9	25.7	20.5
P	n/a	0.9	1.0
S	3.1	0.9	2.2
Cl	0.7	0.5	0.6
K	<0.25	1.2	0.6
Ca	4.0	3.3	3.8
Ti	0.5	0.4	0.4
Cr	n/a	0.1	0.3
Mn	n/a	0.7	0.5
Fe	12.7	9.9	13.6

<sup>1</sup> MPF A3 rock sample "Barnacle Bill", MPF A5 soil sample

The mineralogy presented in Table 4 has not been measured with the past mission directly, but is inferred from the composition by chemical considerations [17]. Assuming that no carbonates, nitrates, or hydrates are in the samples, and that oxygen is assigned stoichiometrically [19], the following mineralogy can be derived:

**Table 4** Mineralogy of samples at the Viking 1 Lander and MPF Lander sites (wt%) [17,19]

	VL1	MPF A3 <sup>(1)</sup>	MPF A5 <sup>(1)</sup>	Calculated "soil-free rock"
Na <sub>2</sub> O	n/a	3.2	2.8	2.6
MgO	8.3	3.0	7.5	2.0
Al <sub>2</sub> O <sub>3</sub>	5.7	10.8	8.7	10.6
SiO <sub>2</sub>	44.7	58.6	47.9	62.0
SO <sub>3</sub>	7.7	2.2	5.6	0.0
K <sub>2</sub> O	<0.3	0.7	0.3	0.7
CaO	5.6	5.3	6.5	7.3
TiO <sub>2</sub>	0.9	0.8	0.9	0.7
Fe <sub>2</sub> O <sub>3</sub> <sup>(2)</sup>	18.2	12.9	17.3	12.0
Cl	0.7	0.5	0.6	0.2

<sup>(1)</sup> MPF A3 rock sample "Barnacle Bill", MPF A5 soil sample

<sup>(2)</sup> Fe<sub>2</sub>O<sub>3</sub> given as FeO with MPF samples

Iron is given in two different oxides in scientific literature: as FeO e.g. in [19] and as Fe<sub>2</sub>O<sub>3</sub> e.g. in [17,20]. Oxidation stages of iron are assigned according to the consideration, that the surface is highly oxidised [20]. A further analysis of surface minerals and iron oxides will be

enabled with instruments installed aboard the two Mars Exploration rovers. These rovers do not only carry an APXS, they also have a Miniature Thermal Emission Spectrometer (Mini-TES) and a Mössbauer Spectrometer (MB) installed [21].

Two example plots derived from Mini-TES and MB measurements are shown below. Utilising data derived with these instruments, a detailed analysis of surface mineralogy is enabled. This will provide a valuable insight about the presence of iron oxides in the surface regolith, which is also required for a thorough prediction of SIR performance utilising resources mined on the surface of Mars.

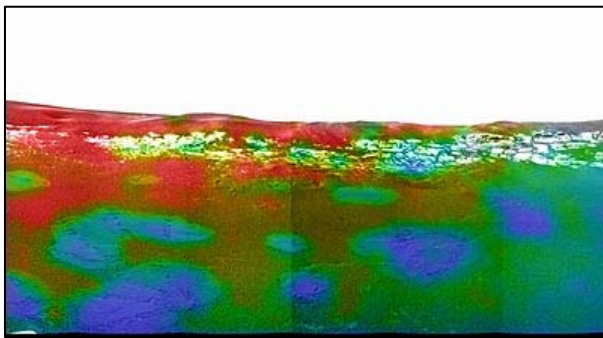


**Figure 8** Data from Opportunity's Mini-TES plotted over a Pancam image of the Meridiani Planum landing site. Red and orange patches indicate high levels of crystalline haematite. Blue and green indicate low levels of the iron-bearing mineral [22]

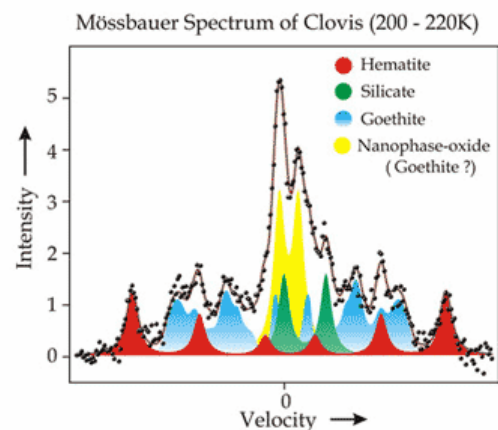


**Figure 9** Mössbauer spectrum showing minerals detected in a rock called "Clovis" in the "Columbia Hills" [23]

### 3.2.3 Fuel and oxygen production on the surface of Mars

The high carbon dioxide content of the Martian atmosphere is particularly interesting with respect to ISRU-based production of oxygen and/or (hydrocarbon-based) fuels. The basic principle applied in generating propellants with state of the art ISRU concepts is derived from the Sabatier reaction, shown in equation E4. Utilising this reaction, methane and water can be produced from a feedstock of hydrogen brought from Earth and carbon dioxide extracted from the ambient atmosphere. This process is applied e.g. with the NASA reference mission ISRU concept [24]. Applying a combined reverse water gas shift (RWGS) / Sabatier reactor, the mass leverage can be increased to values above those achieved with a pure Sabatier process.

Sabatier reaction



Reverse water gas shift reaction (RWGS)



Combined Sabatier / RWGS



Water produced by the process can either be utilised directly (e.g. drinking water) or it can be electrolysed, producing hydrogen that can be fed back into the system, and oxygen that can be stored and used as oxidiser. A simplified schematic of such an ISRU plant is presented in Figure 10.

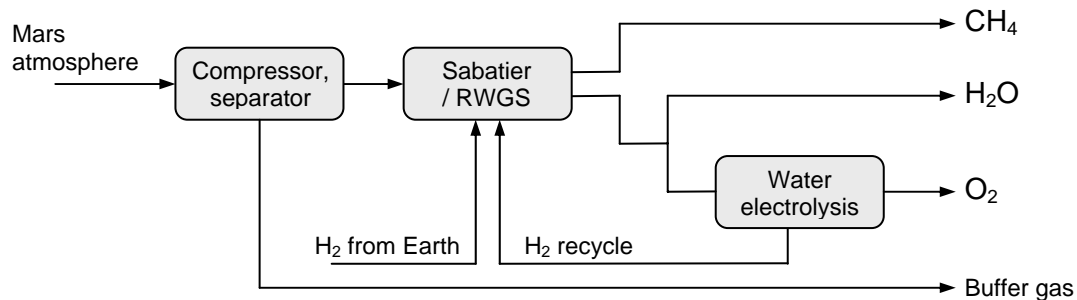


**Figure 10** Basic ISRU system for production of propellants and consumables

Another option discussed with small robotic missions as well as with large manned missions is carbon dioxide decomposition. Decomposition can be achieved with a high-temperature electrolysis cell or by means of a photocatalytic process. The major advantage of this approach is that fuel and oxygen can be produced without relying on a feedstock of species that has to be transported from Earth. Carbon dioxide decomposition is also considered for producing additional quantities of oxygen with the NASA reference mission ISRU system. Thus, carbon dioxide is considered as being the key resource in state of the art ISRU concepts for Mars.

### 3.3 On the utilisation of Lunar and Martian surface materials as contact mass for the sponge iron cycle

The key component of the SIR is the contact mass. Size, porosity, and composition of the pellets determine the performance of the system. Utilising pure iron would theoretically result in the maximum performance per unit of mass. Sintering effects lead to a strong limitation in the effective lifetime of the contact mass, though. The measured surface area of the pellets is already reduced significantly after just a few REDOX cycles due to the aforementioned sintering effects. This results in a continuous deactivation of the contact mass, as the fraction of pellet mass actually involved in the REDOX reactions is gradually

reduced. Sintering effects can be reduced significantly by adding certain minerals, and thus modifying the contact mass composition. In a recent research activity conducted at Graz University of Technology, different “model pellets” were manufactured and tested in order to investigate the effect of contact mass composition on the lifetime performance of the system [5]. In this, the magnetite content of the pellets was varied between 85% and 88%. The silicon dioxide (silica) content was varied between 0 and 10%. An aluminum oxide (alumina) content between 2% and 5% was considered. A calcium oxide (calcia) content between 0 and 10% was considered. Strong sintering effects were derived with samples containing a very low silica content and a high calcia content. Utilising pellets with high silica content and low calcia content proved to reduce sintering effects considerably. The pellets were very stable over the course of the 20 REDOX cycles investigated [5].

If the utilisation of the SIR and/or the RESC process is considered with a mission to Moon or Mars, the contact mass will most likely have to be mined directly from locally available surface resources. Surface regolith on Moon and Mars is highly oxidised and contains large quantities of iron. Regolith contains all three minerals considered with the model pellets -  $\text{SiO}_2$ ,  $\text{Al}_2\text{O}_3$ , and  $\text{CaO}$  – among other minerals not previously investigated with SIR operation. A brief comparison of the range of mineral concentrations investigated with the model pellets, and the range of compositions reported for the samples considered with Table 4 and Table 32 is presented in Table 5 below.

**Table 5** Comparison of mineralogy

	RESC	Mars	Moon
$\text{Fe}_3\text{O}_3$	85-88%	12-18.2%	4.7-19.8%
$\text{Al}_2\text{O}_3$	2-5%	5.7-10.8%	12.0-28.0%
$\text{SiO}_2$	0-10%	44.7-62.0%	40.6-48.1%
$\text{CaO}$	0-10%	5.3-7.3%	10.3-15.8%

The following conclusions can be drawn from the comparison of composition:

- The iron content of the surface materials investigated with the samples of Moon and Mars is significantly lower than with the range of contact masses investigated with the SIR process up to date
- A significantly higher  $\text{SiO}_2$  content has to be considered with Lunar and Martian regolith material. Model pellets with such a high  $\text{SiO}_2$  content would have to be tested in order to analyse the performance with respect to deactivation and sintering effects
- The content of  $\text{Al}_2\text{O}_3$  and  $\text{CaO}$  is in, or slightly above, the range of values considered with the RESC model pellets

For the case of these initial investigations, iron(oxide) is assumed to be the only component participating in the REDOX reaction occurring within the SIR. According to previous

investigations performed with different contact mass compositions,  $\text{SiO}_2$ ,  $\text{Al}_2\text{O}_3$ , and  $\text{CaO}$  are not assumed to be reduced. This assumption is supported by the measurements with the model pellets, that indicate a strong influence of the respective minerals on sintering effects, but not on the REDOX reaction itself. Other components of surface regolith such as  $\text{MgO}$ ,  $\text{MnO}$ ,  $\text{TiO}_2$ ,  $\text{Cr}_2\text{O}_3$ , are assumed to be inactive in the REDOX reactions for the case of these initial investigations. A detailed analysis of SIR performance with Lunar or Martian regolith would have to investigate if - and at what rate - those species actually participate in the REDOX reactions.

### 3.4 Possibilities of SIR/RESC operation in missions to Moon and Mars

The principle of (repeatedly) cycling a contact mass through REDOX reactions can essentially be applied to achieve a number of different objectives. Four major applications, that are of relevance with missions to Moon and Mars, are presented below. The respective applications are investigated in detail within chapters 5 to 8.

Relevant applications of the sponge iron reaction and/or the RESC system are:

- I. Hydrogen production from a ready (hydrocarbon) input species
- II. Oxygen extraction from lunar surface regolith
- III. Hydrogen production with carbon monoxide as SIR reducing agent
- IV. Energy storage

#### Hydrogen production from a ready (hydrocarbon) input species

Hydrogen production from a hydrocarbon source is the primary purpose of the RESC system in terrestrial applications. A hydrocarbon input species can thus be converted into a synthesis gas by means of the built-in reformer unit, applying the SIR as final conversion and gas clean-up step producing very pure hydrogen.

In terrestrial applications, the RESC can be applied to provide a means for on-site hydrogen production. Particularly applications where a limited hydrogen production capacity from a readily available hydrocarbon sources is required are interesting with respect to the operational capabilities of the RESC system. Adding a limited hydrogen production capacity to a regular filling station would therefore be a typical terrestrial application of the system. The same principle could also be applied in space missions. Storing hydrogen efficiently over longer periods of time is still subject to serious limitations. Hydrogen has got a very low volumetric energy density even in liquid state, and boil-off as well as active thermal management have to be considered particularly with the long-term storage required for missions to Mars. Transporting a liquid fuel that can be converted into hydrogen utilising an on-site hydrogen production facility would therefore be a feasible option. The RESC system will be investigated as innovative option for this purpose.

#### Oxygen extraction from lunar regolith

Current scenarios for the production of propellants and/or consumables on the lunar surface are focused on producing oxygen from lunar regolith. This process does not involve a repeated REDOX cycling of the solid volume (primarily dust and smaller particles), but

rather a single oxygen extraction process. The low availability of hydrogen, carbon, and nitrogen in rock samples investigated [25] suggests, that the fuel will be transported from the Earth even if oxygen is produced with ISRU technology.

Thermodynamic limits of extracting oxygen from lunar regolith will be investigated with the sponge iron reactor model developed within this study.

### **Hydrogen production with carbon monoxide as SIR reducing agent**

Carbon monoxide is produced either as by-product or as primary reaction product with many ISRU systems proposed for applications on the surface of Mars. This carbon monoxide gas could either be utilised directly as propellant in a propulsion system or as fuel for a high-temperature fuel cell. Utilising the sponge iron reaction, carbon monoxide could also be utilised as reducing species in a SIR, producing hydrogen as final reaction product. Thus, hydrogen could be produced with a SIR system operated on carbon monoxide as reducing agent.

### **Energy storage**

REDOX reactions of a contact mass could also be utilised as means of storing energy. Iron oxides could be reduced into iron metal and readily stored in cartridges. Hydrogen could be generated on demand by heating the cartridges and feeding steam over the contact mass. Theoretical limits of this storage process are presented in chapter 8.

## 4 Mathematical modelling of the RESC plant

A mathematical model of the complete RESC cycle has been developed for system analysis and performance prediction. The model essentially consists of a hydrocarbon reformer model that is capable of calculating mass and energy balances for an isothermal hydrocarbon reforming reaction, a mathematical model of the SIR in oxidation and reduction mode, and an integration model where the different sub-models are implemented along with simplified models of heat exchangers, burners, and gas mixing units. Derivation and implementation of the individual component models is briefly discussed in the following chapter.

### 4.1 Aim of the mathematical model

The basic feasibility of the RESC concept has been proven in a laboratory-scale test unit that has been successfully operated at Graz University of Technology with different hydrocarbon fuels. The next step in the investigations was thus to develop a mathematical model of the complete hydrogen production plant in order to analyse the possibilities and the limitations of the overall process. Key performance parameters were to be computed, investigating mass and energy balances of the individual components as well as of the overall process. The model that has been developed is based on a pure thermodynamic analysis, computing the thermodynamic limits of the idealised process. The performance figures presented in the following can thus be referred to as ideal thermodynamic limits of the process. The actual performance of a RESC plant would necessarily be worse than the figures derived for the ideal process considered with the model development, particularly if a small laboratory-scale unit is investigated. The model nevertheless provides a good overview about governing aspects of RESC design, operation, and overall efficiency.

### 4.2 Mathematical modelling of the hydrocarbon reformer

#### 4.2.1 Introduction to mathematical modelling of the hydrocarbon reformer

The first component model discussed is the hydrocarbon reformer unit model. This mathematical model is utilised to compute the reformer output gas concentrations as well as the thermal balance for a specific input gas composition supplied to the reformer. Governing equations of the reformer model are presented below, along with a brief overview of mathematical implementation and model performance. The full RESC model is based on applying a pre-reformer unit – particularly if higher hydrocarbons are considered – and a main reformer unit. Both reformers are mathematically described with the same set of equations, allowing to manually assign the operating temperature levels of either reformer unit.

#### 4.2.2 Governing equations of the reformer model

The governing equations describing the reforming reaction of a hydrocarbon fuel with steam and/or carbon dioxide are written in equations E7 and E8. Reforming of hydrocarbons is usually performed at elevated temperatures under the presence of catalyst materials, converting the hydrocarbon fuel supplied into a hydrogen- and/or carbon monoxide-rich

reformer output gas stream. The water gas shift reaction written in equation E9 has also got to be considered with a complete thermodynamic analysis of the hydrocarbon reformer.

Hydrocarbon reforming reaction



Water gas shift reaction



The steam reforming reactions E7 and E8 as well as the water-gas-shift reaction E9 proceed very rapidly at temperatures of 500°C and above. It can thus be assumed that the synthesis is close to equilibrium at the reformer outlet, presuming a sufficient dwell time of the gas in the reformer bed. Rostrup-Nielsen [26,27,28,29], Barin et al. [30], and Christensen [31] came to the same conclusions in their analyses.

#### 4.2.3 Implementation of the hydrocarbon reformer model

The hydrocarbon reformer model implemented with the RESC simulation is based on the assumption of an isothermal reforming reaction. Thus, the reformer is continuously heated by the lean gas burner unit to avoid a reduction in operating temperature along the gas flow direction due to the endothermic reforming reaction. The heat flux between reformer unit and ambient is neglected. Output gas compositions are furthermore assumed to be in full equilibrium for the reforming temperature specified.

Equilibrium composition of the synthesis gas at a specified temperature and pressure are determined by applying the concept of minimising Gibbs energy. This method was developed at NASA [32] and has been demonstrated for thermodynamic equilibrium computations of numerous chemical systems. The main advantage of the Gibbs minimisation technique is its great flexibility and extensibility. The governing principle of this method is the fact, that the Gibbs energy reaches a minimum if a system is in thermodynamic equilibrium. The Gibbs energy  $G$  (J) of a system containing a number of  $NS$  species is a function of temperature  $T$  (K), pressure (Pa), and system composition, where  $n_i$  is the number of moles of species  $i$  as shown in equation E10.

$$G = f(T, p, n_1, \dots, n_{NS}) \quad (E10)$$

It is thus necessary to compute the global minimum of function E10 for the solution of the Gibbs minimisation problem. If system temperature and pressure are assumed to be known and constant, the Gibbs energy is solely a function of system composition. Thus, the minimisation problem is simplified to finding the gas composition with the smallest Gibbs energy as shown in equation E11. Thermodynamic data for the reformer model calculations was taken from tables presented in Barin [33].

$$G = f(n_1, \dots, n_{NS}) \quad (E11)$$

#### 4.2.4 Example calculation of the hydrocarbon reformer model

Figure 11 shows an example output plot of the hydrocarbon reformer model, assuming an input flux of one mole of methane, steam, and carbon dioxide, each. Figure 12 shows the equilibrium gas compositions for supplying five moles of steam and five moles of carbon dioxide for each mole of heptane. The output gas composition is shown as a function of equilibrium temperature. Assuming a reformer output temperature in the range of 800°C – which is a normal RESC process temperature – heptane is completely converted, and only minor traces of methane remain in the reformer output gases. These traces of methane are combusted in the lean gas burner, and the energy is subsequently utilised for heating purposes within the RESC.

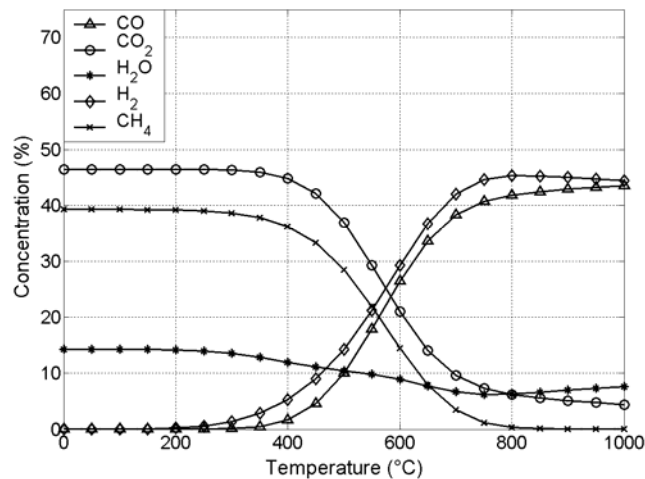


**Figure 11** Example output plot of the reformer model; input gas composition: one mole  $\text{CH}_4$ , one mole of  $\text{CO}_2$ , and one mole of  $\text{H}_2\text{O}$

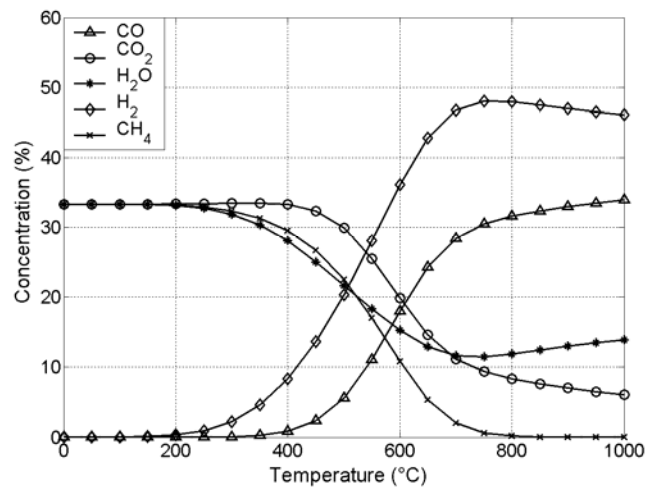


**Figure 12** Example output plot of the reformer model; input gas composition: one mole of  $\text{C}_7\text{H}_{16}$ , five moles of  $\text{CO}_2$ , and five moles of  $\text{H}_2\text{O}$

## 4.3 Mathematical modelling of the Sponge Iron Reactor (SIR)

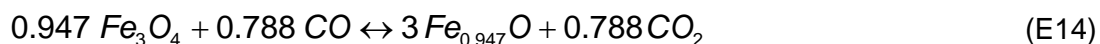
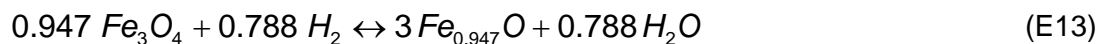
### 4.3.1 Introduction to mathematical modelling of the sponge iron reaction

The sponge iron reaction is utilised as core hydrogen production process by reducing and subsequently oxidising pellets to and from the magnetite/wuestite/iron stages. Mathematical modelling of the SIR is based on determining the equilibrium gas concentrations of hydrogen and steam as well as of carbon monoxide and carbon dioxide as a function of temperature, input gas concentrations, and oxidation stage of the contact mass. Other gases, particularly hydrocarbons, are assumed to pass through the reactor without oxidising and/or reducing the pellets. Measurements performed with the laboratory-scale RESC unit at Graz University of Technology demonstrated that this assumption is valid, and that the outlet gases can be considered being in full equilibrium with the range of temperatures investigated for potential RESC operation. Reduction of the pellets is assumed to proceed with hydrogen and carbon monoxide in parallel, achieving a full equilibrium with each species. Wuestite is not considered in the stoichiometric ratio (FeO) but rather as  $Fe_{0.947}O$ , which represents a common composition of wuestite.

### 4.3.2 Governing equations of the sponge iron reactor model

The first governing equation of the SIR is the reaction between magnetite and wuestite written in equation E13, producing three moles of wuestite out of 0.947 moles of magnetite. A total of 0.788 moles of hydrogen are converted into steam by this reaction. The same reaction can also proceed with carbon monoxide as reducing species according to equation E14, producing 0.788 moles of carbon dioxide as gaseous reaction product, respectively.

Magnetite-wuestite reaction



The second reaction considered with the SIR model is the conversion of wuestite into iron according to equation E15. This reaction produces 0.947 moles of iron metal out of one mole of wuestite by converting one mole of hydrogen into steam. Conversion of wuestite into iron can also proceed with carbon monoxide as reducing species according to equation E16.

Wuestite-iron reaction



The haematite ( $Fe_2O_3$ ) to magnetite equilibrium was considered with initial investigations of the SIR hydrogen production capability. Laboratory investigations revealed, that this oxidation stage can be neglected because the pellets could not be oxidised back into the

haematite stage. Haematite is therefore not included with this thermodynamic analysis of the RESC process.

The Baur-Glaessner diagram shown in Figure 13 provides an overview about the correlation between iron metal, wuestite, magnetite, and the respective equilibrium gas concentrations of carbon dioxide and steam. The equilibrium gas concentrations  $y^*$  (in vol.-%) are derived from the individual gas concentrations  $y$  (vol.-%) according to equations E17 and E18.

$$y_{H_2O}^* = \frac{y_{H_2O}}{(y_{H_2} + y_{H_2O})} \quad (E17)$$

$$y_{CO_2}^* = \frac{y_{CO_2}}{(y_{CO} + y_{CO_2})} \quad (E18)$$

The Baur-Glaessner diagram shows the respective equilibrium concentrations, with the steam/hydrogen equilibria shown as dash-dot lines, and the carbon dioxide/carbon dioxide equilibria shown as solid lines. The two equilibrium lines shown on the left hand side of the plot represent the iron/wuestite equilibria, whereas the lines on the right hand side represent the wuestite/magnetite equilibria. Thus, the equilibrium gas concentrations can be derived from the Baur-Glaessner diagram as a function of reaction temperature if the input gas composition is known.

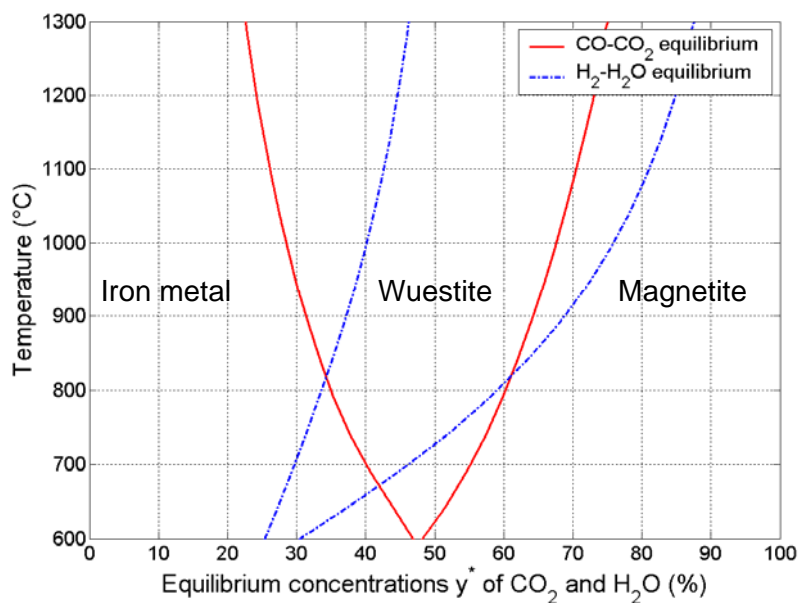


**Figure 13** Baur-Glaessner diagram

### 4.3.3 Implementation of the sponge iron reactor model

Implementation of the SIR is based on computing the equilibrium concentrations for the iron/wuestite and the wuestite/magnetite equilibrium for the stream of input gases supplied to the reactor. In this, the following assumptions are applied:

- Hydrocarbons are assumed to be inactive within the SIR, and thus do not participate in the reduction and oxidation of the pellets
- Reduction of the pellets is assumed to proceed with hydrogen and carbon monoxide in parallel, achieving a full equilibrium with either species.
- SIR output gases are assumed to be in the full equilibrium with the respective iron(-oxides)
- Iron(-oxide) pellets are assumed to be present as wuestite, magnetite, and pure iron, only
- The SIR is computed as isothermal process

The SIR can be considered as an isothermal process if the amount of heat consumed and/or produced by the reaction of iron pellets with the gas phase is fully transferred into or transported out of the reactor, respectively. A RESC plant configuration where at least two individual SIRs are operated in parallel with one SIR in oxidation mode and the other SIR in reduction mode therefore suggests itself. Thus, the heat produced by the reactor with the exothermic reaction can be directly transferred into the other reactor operated with an endothermic reaction by means of thermal conduction. The inevitable difference between the operating temperatures of the SIR operated in reduction and the one operated in oxidation mode is neglected with this initial investigation of RESC performance. Thermodynamic data was again taken from tables presented in Barin [33]. Once the output gas concentrations have been derived, the thermal balance of the SIR is computed. This thermal balance is again based on the assumption of an isothermal process. The heat flux required to maintain a constant SIR operating temperature for the individual reactors is calculated. The change in enthalpy for the reactions from magnetite to wuestite, and from wuestite to iron is computed from the values of the enthalpy of formation.

## 4.4 Mathematical modelling of the complete RESC plant

### 4.4.1 Auxiliary devices required in a RESC plant

A number of auxiliary devices is required to handle the stream of gases and to transfer heat between the different gas streams within the RESC plant. Evaporators are installed to transfer liquid hydrocarbon fuels into the gas phase before they are mixed with the recycle gas stream in reduction mode, and to produce steam from liquid water in the oxidation mode. These evaporators are included in the thermodynamic analysis by calculating the heat flux required to achieve the change in enthalpy required. Heat exchangers are also utilised to transfer heat from the lean gas into the input gases, and are calculated in the

same way. Burner units are required to combust the lean gas, and to provide an additional heat source in the RESC oxidation mode. These burner units are again considered with a thermodynamic analysis, utilising air as oxidiser. Two components are of special importance with the reduction mode: gas mixer and recycle valve. The fraction of SIR offgas that is recycled and added to the hydrocarbon fuel supplied is determined by the recycle valve. This hot recycle gas stream is added to the input stream of hydrocarbon fuel in the gas mixing unit. Both devices are calculated by applying a straight-forward mass and energy balance. Pumps and compressors required for driving species through the plant are neglected. The whole plant is assumed to be operated at ambient pressure.

#### 4.4.2 Overview of the RESC process in reduction mode

Figure 14 shows a schematic of the RESC plant operated in reduction mode. Hydrocarbon fuel is supplied to the system as input species. An optional evaporator unit is included if liquid input species (e.g. higher hydrocarbons) are utilised as fuel. The hot recycle gas stream is added to this flux of input hydrocarbons before the mixture of gases is heated to process temperature and supplied to the isothermal reformer unit. The hydrocarbon reformer (or the main hydrocarbon reformer in case a pre-reformer unit is installed, respectively) is operated at RESC process temperature. Reformer as well as SIR are thus operated at the same temperature level, which strongly simplifies thermal management of the system, and leads to a high conversion rate of the hydrocarbon fuel within the reforming reaction due to the elevated reforming temperatures that are applied. SIR offgas is divided into a fraction that is recycled and added to the input gas stream, and the remaining fraction, the so-called lean gas, that is fed into a burner unit. Lean gas is thus combusted with oxygen (or air in terrestrial applications), and the thermal energy produced is utilised to heat up the hydrocarbon feed and the reformer input gases.

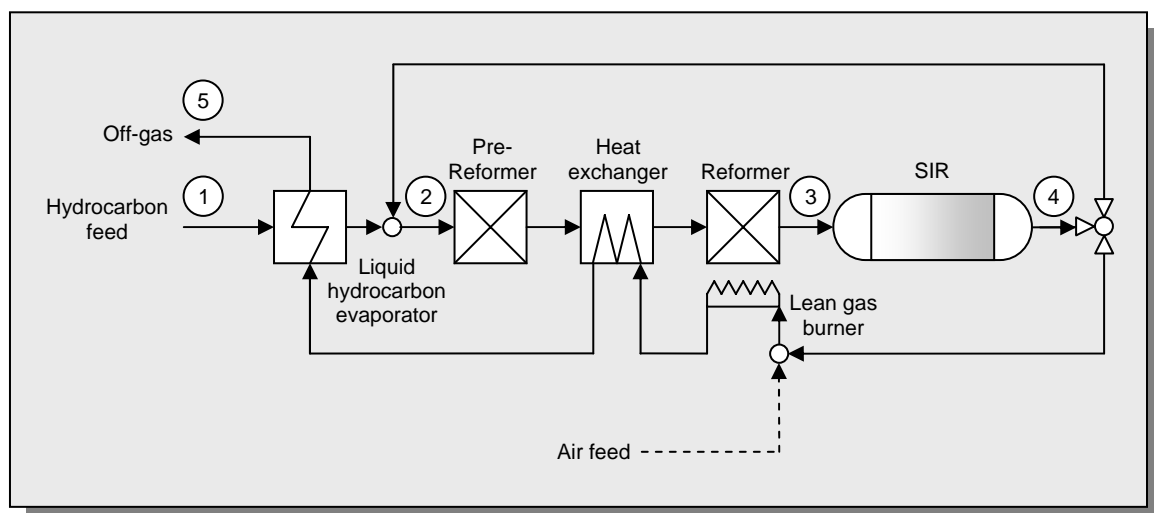


**Figure 14** Schematic of the RESC process in reduction mode

#### 4.4.3 Overview of the RESC process in oxidation mode

Operating the RESC in oxidation mode requires less auxiliary equipment than operation in reduction mode. Figure 15 shows a schematic of the RESC plant layout in oxidation mode. Liquid water is supplied to the RESC at ambient temperature. This water is evaporated and heated up to process temperature before it is fed into the SIR. The hot SIR offgas is utilised to heat the input water in the evaporator and in heat exchanger 1 (HEX1), whereas heat exchanger 2 (HEX2) is installed to add additional heat coming from an optional hydrocarbon burner unit. This hydrocarbon burner unit is assumed to be operated with the same hydrocarbon fuel that is also used as input species for the RESC process. If an integrated RESC plant is considered where at least one SIR is operated in oxidation mode and a different SIR operated in reduction mode, the installation of an additional hydrocarbon burner unit could be avoided by injecting fresh hydrocarbon fuel into the lean gas burner unit. Thus, the additional thermal energy could be supplied to the system without installing two separate burner units. Energy balance and efficiency of the overall process are identical in both cases, assuming that fuel and oxygen are supplied at the same temperatures, and that the reaction products are removed with the offgas at the same temperature.

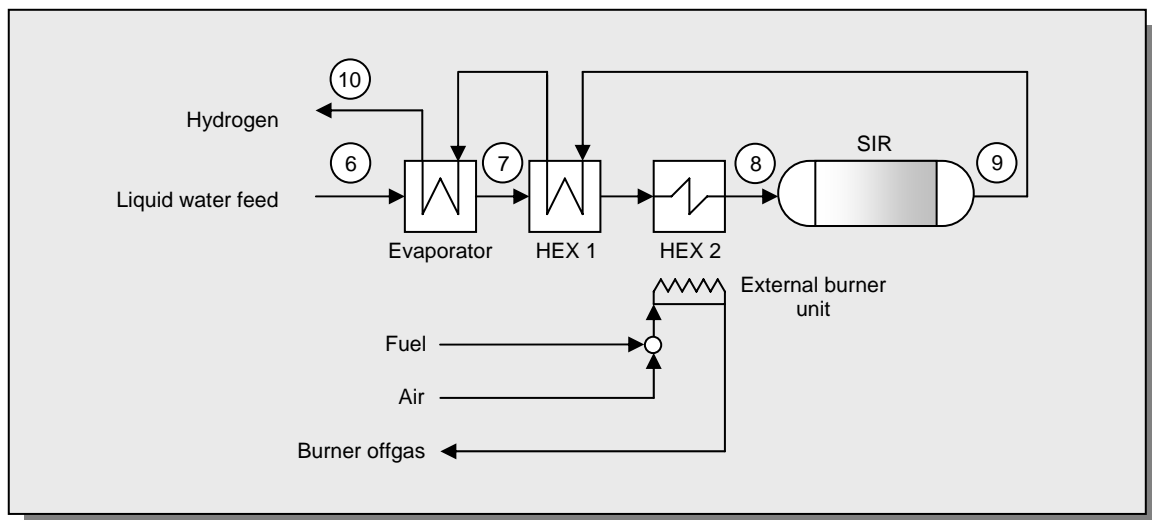


Figure 15 Schematic of the RESC process in oxidation mode

#### 4.4.4 Input species considered with the RESC simulation

The RESC can essentially be operated with a wide range of different input species produced from fossil as well as from regenerative sources. The only requirement, that potential RESC input species have to meet is, that the species can be converted into a hydrogen and/or carbon monoxide-rich synthesis gas. Performance of the RESC system operated with the range of input species presented in Table 6 is investigated within this study. Four categories of hydrocarbons are considered. Methane ( $\text{CH}_4$ ) is not only one of the primary sources of hydrogen in state-of-the-art terrestrial hydrogen production processes - due to the wide availability of natural gas - but is also one of the primary fuel

options considered with ISRU on Mars. Liquid petroleum gases (LPGs) are an interesting option for terrestrial on-site hydrogen production because they are widely available, and they can be easily transported in low-pressure vessels. LPGs are even considered as direct fuel option for passenger vehicles operated primarily in small fleet operation. LPGs are included in this initial survey on RESC system performance although they are not considered being a primary fuel option for space applications. Propane (C<sub>3</sub>H<sub>8</sub>) and Butane (C<sub>4</sub>H<sub>10</sub>) are investigated with the analysis presented in the following. The third category of hydrocarbons investigated are liquid higher hydrocarbons. Heptane (C<sub>7</sub>H<sub>16</sub>) and Octane (C<sub>8</sub>H<sub>18</sub>) are considered. Both have a strong relevance with terrestrial transportation applications; Heptane has also been applied in investigations performed with the laboratory-scale RESC unit operated in the Christian-Doppler Laboratory for Fuel Cell Systems. Higher hydrocarbons are an option for space missions because they can be easily transported and stored without requiring the complex storage techniques required for cryogenic hydrogen storage, for instance. Alcohol fuels are the fourth category of RESC input species investigated within this project. Methanol and ethanol are relevant for terrestrial and space applications, combining the advantage of simple storage technology with the ability to produce hydrogen in compact low-temperature reformers. Methanol can also be utilised directly with a direct methanol fuel cell.

**Table 6** Overview of potential RESC input species covered within the initial investigations

Formula	Hydrocarbon	Standard state
<i>Reference input species</i>		
CH <sub>4</sub>	Methane	gaseous
<i>Liquefied petroleum gases (LPGs)</i>		
C <sub>3</sub> H <sub>8</sub>	Propane	gaseous <sup>1)</sup>
C <sub>4</sub> H <sub>10</sub>	Butane	gaseous <sup>1)</sup>
<i>Higher hydrocarbons</i>		
C <sub>7</sub> H <sub>16</sub>	Heptane	liquid
C <sub>8</sub> H <sub>18</sub>	Octane	liquid
<i>Alcohol fuels</i>		
CH <sub>3</sub> OH	Methanol	liquid
C <sub>2</sub> H <sub>5</sub> OH	Ethanol	liquid

<sup>1)</sup> can be liquefied at ambient temperature with small pressures

Considering a space mission where the fuel is not produced on the surface of Moon or Mars, the issue of fuel storage and transportation efficiency is of special interest. The range of potential RESC input gases is investigated with respect to the gravimetric and volumetric energy storage density in Table 7. Only the liquid (cryogenic) state is considered due to the limitations in storage volume. Hydrogen and carbon monoxide are included for comparison.

**Table 7** Bulk data of RESC input species investigated

	Density <sup>1</sup>	Boiling temperature <sup>1</sup>	Gravimetric energy density <sup>2</sup>	Volumetric energy density
	kg/m <sup>3</sup>	°C	MJ/kg	MJ/liter
Hydrogen (liquid)	71	-252.8	120	9
Carbon monoxide (liquid)	789	-191.6	10	8
Methane (liquid)	423	-161.6	50	21
Propane (liquid)	582	-42.1	46	27
Butane (liquid)	601	-0.5	46	27
Heptane	680	98.0	44	30
Octane	700	126.0	45	31
Methanol	790	64.5	20	16
Ethanol	790	78.0	27	21

<sup>1</sup>Derived from MSDS, airtiquide, <http://www.us.airliquide.com/en/business/msds/category/pure.asp>

<sup>2</sup>Derived from W.Beitz, K.-H. Grote, Dubbel, 19th ed., Springer, 1997

Higher hydrocarbons considered with this investigation (heptane and octane) offer the best overall performance with respect to storage volume and mass. The elevated boiling temperatures of the two higher hydrocarbons furthermore enable storage and transport in light vessels without facing the problems and limitations of active temperature control and boil-off faced with cryogenic hydrogen storage, for instance.

#### 4.4.5 Example calculation performed with the RESC model

An example calculation of the full RESC simulation is described in the following sub-section. Typical operation of two reference cases is presented, comparing characteristic key performance data for the RESC operated with methane (CH<sub>4</sub>) and data generated for heptane (C<sub>7</sub>H<sub>16</sub>) fuel. Governing simulation parameters are assigned according to the values presented in Table 8.

**Table 8** RESC simulation parameters, reference case

Reformer temperature	800°C
SIR temperature	800°C
Input species temperature	25°C
Liquid water input temperature	25°C
Offgas temperature	150°C
Evaporator temperature <sup>1)</sup>	150°C
System pressure	1 bar
Recycle rate	50%

<sup>1)</sup> for liquid hydrocarbon evaporator (reduction mode) and liquid water evaporator (oxidation mode)

Variation of the molar flux of species for five different points in the reduction mode of the RESC is presented in Table 9. In this, the five conditions refer to points one to five in Figure 14. *Feed* refers to the hydrocarbon species that is supplied as fuel. *After mixing* refers to the condition after mixing the fresh hydrocarbon fuel and the recycle gas stream. *Reformer output* refers to the gas mixture that is coming out of the reformer unit. *SIR output* refers to the SIR offgas, and *Offgas* refers to the lean gas leaving the RESC after being combusted in the burner unit and cooled down in the system of heat exchangers.

**Table 9** Overview of the molar flux of species within the reduction cycle of the RESC per mole of methane fuel supplied (recycle rate is 0.5, process temperature is 800°C)

	Feed	After mixing	Reformer output	SIR output	Offgas
H <sub>2</sub>	0.00	0.81	3.45	1.62	0.00
H <sub>2</sub> O	0.00	1.17	0.51	2.34	2.00
CO	0.00	0.39	1.71	0.79	0.00
CO <sub>2</sub>	0.00	0.60	0.27	1.19	1.00
CH <sub>4</sub>	1.00	1.01	0.02	0.02	0.00

The values given are dimensionless and present the number of moles of species per mole of methane fuel. The reduction in the flux of hydrogen and carbon monoxide between reformer output and SIR output corresponds to the reduction of iron oxides by oxidation of the gaseous species. The offgas composition resembles the hydrocarbon fuel plus the oxygen required to burn the synthesis gas in the lean gas burner unit. Table 10 gives an overview of the molar fluxes with heptane as input species. Significantly larger fluxes are derived per mole of heptane fuel due to the fact that reforming of heptane produces fifteen moles of synthesis gas and approximately the same quantity of hydrogen if the synthesis gas is utilised for contact mass reduction in the SIR, whereas reforming of methane generates only three moles of synthesis gas. The fraction of hydrogen and carbon monoxide utilised for reducing the pellets is similar to the value derived for the methane-fuelled RESC (57.0% of hydrogen and carbon monoxide are utilised with the heptane-fuelled RESC compared to 53.4% with the methane-fuelled RESC). A detailed analysis on the utilisation of hydrogen and carbon monoxide within the SIR is given in section 5.1.4.

**Table 10** Overview of the molar flux of species within the reduction cycle of the RESC per mole of heptane fuel supplied (recycle rate is 0.5, process temperature is 800°C)

	Feed	After mixing	Reformer output	SIR output	Offgas
H <sub>2</sub>	0.00	3.15	14.48	6.31	0.00
H <sub>2</sub> O	0.00	4.56	0.95	9.13	8.00
CO	0.00	2.72	12.82	5.45	0.00
CO <sub>2</sub>	0.00	4.13	0.89	8.27	7.00
C <sub>7</sub> H <sub>16</sub>	1.00	1.00	0.00	0.00	0.00

Deriving the thermal energy balance for the RESC is of special importance with respect to the conversion efficiency of hydrocarbon fuel into hydrogen. The thermal energy balance for methane and heptane fuel is presented in Table 11 for the reduction cycle of the RESC.

**Table 11** Overview of temperatures and thermal energy balance for the reduction cycle of the RESC

	Methane fuel		Heptane fuel	
	Temperature (°C)	Heat balance (kJ)	Temperature (°C)	Heat balance (kJ)
Hydrocarbon feed	25	0	25	0
Evaporator	-	0	150	61
Gas mixing	568	0	587	0
Heat exchanger	800	44	800	209
Reformer <sup>1)</sup>	800	235	800	1261
SIR	800	36	800	129
Offgas heat extraction	150	-387	150	-2010
Energy balance reduction	-	-73	-	-350

The values are again calculated per mole of hydrocarbon fuel supplied. According to the values derived, the reduction cycle is mildly exothermic in both cases. The heat that can be drawn out of the hot lean gas after combusting it in the burner unit with oxygen is slightly larger than the heat that is required to heat the gases to process temperature, and to run the SIR in reduction mode.

The thermal energy balance of the RESC operated in oxidation mode is presented in Table 12. The five conditions shown in the table refer to points six to ten in Figure 15. *Water feed* refers to the liquid water that is supplied to the RESC process, *Evaporator* refers to the energy balance of the water evaporator unit, *Heat exchanger* represents gas conditions after the heat exchangers, which also corresponds to the SIR input conditions. *SIR* refers to the SIR reactor outlet conditions, and *Offgas heat extraction* refers to the RESC process offgas conditions. A considerable amount of energy is thus required for evaporating the water, and heating the steam up to process temperature. Offgas heat extraction can only provide a fraction of the total amount of thermal energy required. Operating the RESC in oxidation mode is therefore endothermic, consuming more energy than the exothermic reduction cycle can provide. This explains why the additional hydrocarbon burner unit shown in Figure 15 has to be installed.

**Table 12** Overview of process temperatures and thermal energy balance for the oxidation cycle of the RESC

	Methane fuel		Heptane fuel	
	Temperature (°C)	Heat balance (kJ)	Temperature (°C)	Heat balance (kJ)
Water feed	25	-	25	0
Evaporator	150	200	150	1131
Heat exchanger	800	103	800	581
SIR	800	-67	800	-380
Offgas heat extraction	150	-88	150	-495
Energy balance oxidation	-	148	-	837

The overall RESC thermal energy balance is positive in case of methane as well as in case of heptane fuel. In both cases, a net input of heat is thus required to maintain the temperature levels assigned. This additional energy could be supplied by electric heaters – as it is done with the small laboratory-scale RESC device operated at Graz University of Technology – or by burning additional hydrocarbon fuel. Considering a stand-alone RESC unit for on-site hydrogen production, this required heat could be generated by burning additional quantities of the same hydrocarbon fuel already utilised with the hydrogen production process. This additional fuel consumption must be considered in an overall energy balance of the RESC system, which results in a significant reduction of the overall hydrocarbon to hydrogen conversion efficiency.

## 5 Applying the RESC for hydrogen production from a ready hydrocarbon input species

Applying the RESC as a means of converting a ready input species (e.g. gaseous and liquid hydrocarbons, alcohols) into pure hydrogen is investigated in the following chapter. Results of the mass and energy balance calculations are discussed along with the overall RESC system conversion efficiency.

### 5.1 Mass balance of the conversion process

The first issue discussed within this chapter is the mass and energy balance of the RESC as a function of input species. Example calculations performed with methane and heptane as input species are presented in detail within the first subsections of this chapter. A general mass balance is subsequently presented for each of the RESC input species considered.

Key parameters in RESC operation with methane and heptane are presented and compared in the following section. In order to provide a compressed overview of the performance, the plots are limited to a reduced range of operating parameters. The investigated range of operating temperatures is 750°C-1000°C for both species, and a

recycle rate between 40% and 80% is applied with methane fuel, and 55% to 80% with heptane fuel. Lower temperatures and smaller recycle rates are not considered due to the low conversion efficiencies achieved. Higher temperatures and larger recycle rates are not investigated due to limitations in plant size and material properties.

### 5.1.1 RESC hydrogen production capability

One of the key figures applied in describing the RESC hydrogen production capability is the number of moles of hydrogen produced per mole of hydrocarbon fuel supplied. Figure 16 provides an overview of the hydrogen production capability for the RESC operated with methane and heptane fuel. In this, the amount of fuel consumed for additional heating purposes is neglected. Considering only the amount of fuel that is actually supplied to the RESC reformer is particularly interesting with respect to the fact that the additional heat required to run the process could also be supplied by utilising waste heat of a different process (e.g. a nuclear power plant). Higher process temperatures and higher recycle rates generally lead to an increase in the hydrogen production capability.

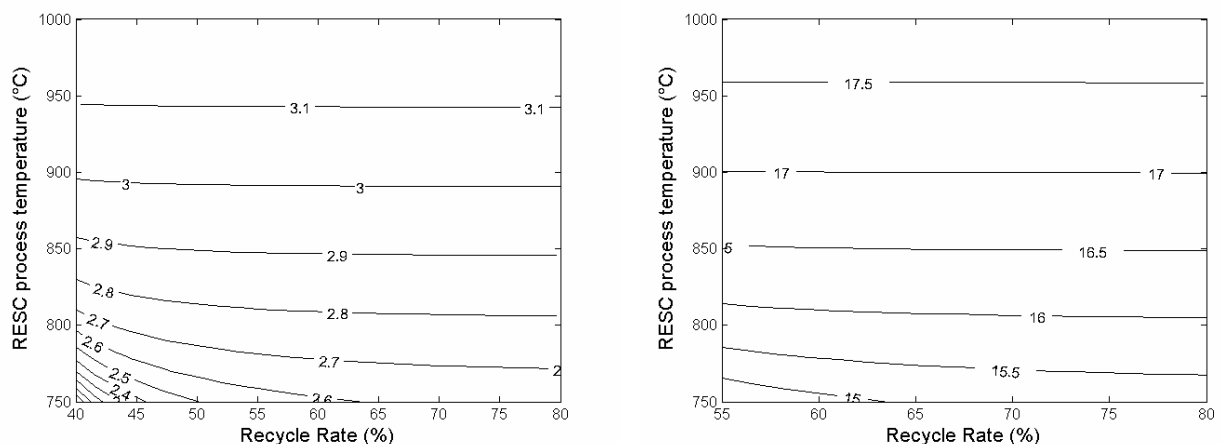


**Figure 16** Moles of hydrogen produced per mole of methane (left) and heptane (right) supplied to the system

### 5.1.2 Additional hydrocarbon fuel required for heating purposes

The fraction of fuel that is required for heating purposes in the hydrocarbon burner units is presented in Figure 17. This assumes, that the additional heat required for the endothermic RESC process is derived by combusting an additional input stream of some of the methane or heptane fuel utilised with the RESC process, respectively.

Operation at elevated temperatures requires a significant amount of energy primarily to heat the input gases to process temperature. Roughly a quarter of the RESC fuel is thus required for additional heating purposes with methane as well as with heptane fuel with the maximum process temperature of 1000°C investigated. A large fraction of this thermal

energy is stored in the RESC process gases, but additional heating nevertheless causes a reduction in the overall fuel-to-hydrogen conversion efficiency.

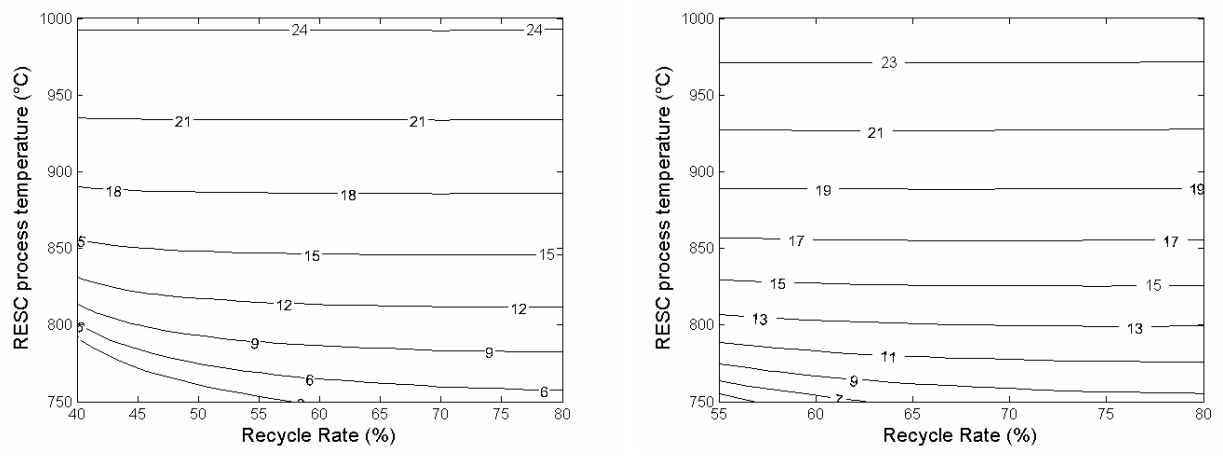


**Figure 17** Fraction of total methane (left) and heptane (right) consumption required for heating purposes (%)

### 5.1.3 Overall molar flux supplied to the SIR

Large recycle rates result in large volumes that have to be moved through the different stages of the RESC. A careful evaluation between an increase in process efficiency and a reduction in plant size has to be made in order to derive a compact setup that can be operated efficiently. Figure 18 shows the variation of SIR input molflux per mole of hydrocarbon fuel supplied. Increasing the recycle rate from 50 to 75% doubles the molflux, implying that the reactor as well as the tubing has to be designed either twice as large, or that the gas velocity is twice as large. Similar values are also derived for the heptane-fuelled RESC plant as shown.

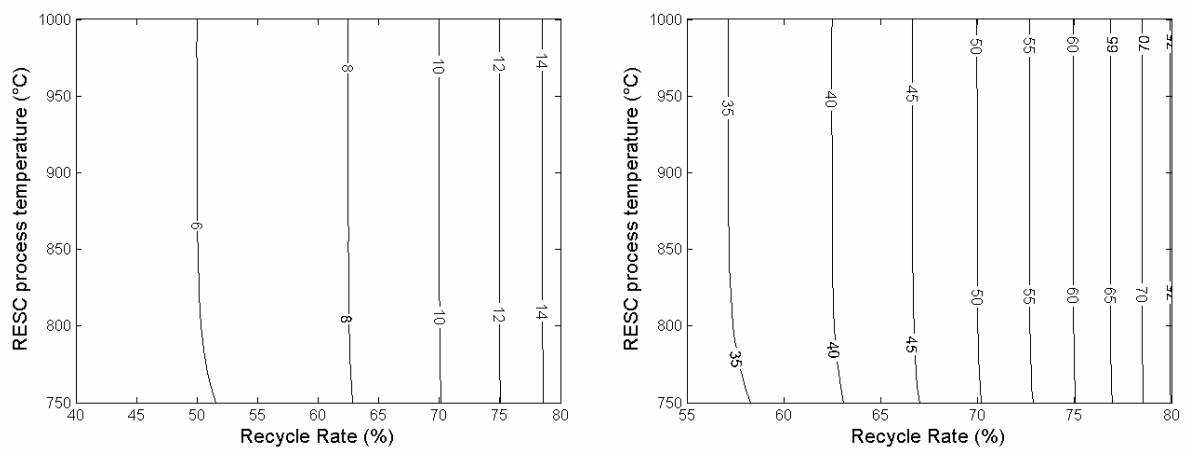


**Figure 18** Molar flux supplied to the SIR in case of methane (left) and heptane (right) fuel

### 5.1.4 Fuel utilisation of the SIR as a function of operating condition

An interesting aspect in SIR operation is investigated in Figure 19. The plots show the fraction of hydrogen and carbon monoxide supplied to the SIR that is utilised for reducing iron oxides. This fraction is generally quite low, being in the order of 30-70% for the range of operating conditions considered. High recycle rates lead to particularly low rates of utilisation due to the thinning of the reducing gases with steam and carbon dioxide. Low rates of utilisation show the strong importance of utilising SIR output gases as heat source for the reforming reaction. Thus, the energy of hydrogen and carbon monoxide that is not utilised in the SIR is not lost for the process, but is applied to produce additional amounts of hydrogen and carbon monoxide in the reformer unit.

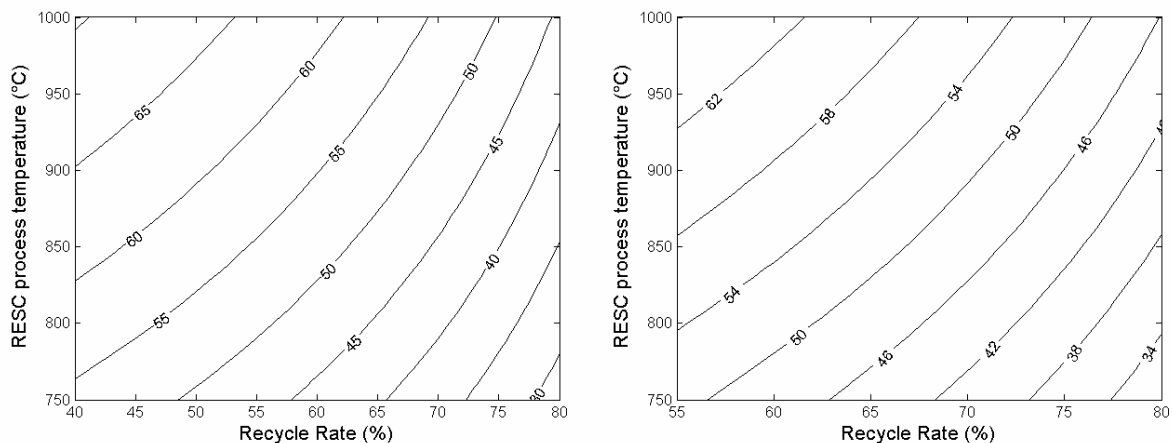


**Figure 19** Fraction of carbon monoxide and hydrogen supplied to the SIR that is utilised for iron oxide reduction in case of methane (left) and heptane (right) input gas (%)

### 5.1.5 Mass balance of the input species considered

A mass balance for each of the fuel options investigated within this study is presented in Table 13. In the first column – denoted *SIR input* – it is presented, how many moles of species are supplied into the sponge iron reactor per mole of input gas supplied. High values are derived particularly for higher hydrocarbons, where one mole of input gas is converted into a large number of moles of synthesis gas within the hydrocarbon reformer unit. The second column – denoted *Fraction of SIR gases utilised* - gives the fraction of reducing gases ( $H_2$ ,  $CO$ ), that is utilised in the reduction of contact mass. Large values are again derived for higher hydrocarbons. Low rates of utilisation are derived for methanol and ethanol, where high quantities of oxidised species (steam/carbon dioxide) are produced in the reforming process, which in turn limits the reduction capacity within the SIR. The third column – denoted *Hydrogen production* - presents how many moles of hydrogen can be produced per mole of input species supplied (one hydrogen molecule can be produced for each oxygen atom removed from the contact mass). The last column presents how many moles of hydrogen can be produced by each mole of SIR input gas. High values imply, that hydrogen can be produced with small volumes (i.e. small flow rates in the system), whereas

small values refer to large diameters and large quantities of gas that have to be moved in the system. Large ratios of hydrogen production are therefore desired in order to keep the system volume small, and to provide a compact hydrogen production system package.

**Table 13** Compressed mass balance for the investigated input gases

	SIR input	Fraction of SIR gases utilised	Hydrogen production	Ratio of H <sub>2</sub> /SIR input gases
	mol/mol <sub>input</sub>	%	mol <sub>H<sub>2</sub></sub> /mol <sub>input</sub>	mol <sub>H<sub>2</sub></sub> /mol <sub>SIR</sub>
Methane	5.95	53.42	2.75	0.46
Propane	13.80	55.98	7.04	0.51
Butane	17.71	56.39	9.17	0.52
Heptane	29.43	56.96	15.55	0.53
Octane	33.33	57.06	17.68	0.53
Methanol	5.99	42.33	1.78	0.30
Ethanol	9.97	49.59	3.95	0.40

The gravimetric and volumetric hydrogen production capacity per unit of mass and per unit of volume of input species is one of the key figures in performance evaluation of the input species options. A compressed overview of the values derived for the seven input species considered is shown in Table 14. Values presented in the gravimetric transport efficiency column indicate, how many kilograms of hydrogen can be produced out of each kilogram of input species. Thus, 0.35 kg of hydrogen can be produced out of each kg of methane that is supplied to the RESC plant, for instance.

Methane, LPGs, and higher hydrocarbons offer a gravimetric conversion efficiencies in the order of 30-35%. Alcohols have a very low gravimetric conversion efficiency, being significantly lower than with the other species considered. The best volumetric conversion efficiency is derived for higher hydrocarbons. More than three liters of liquid hydrogen can be produced out of each liter of fuel. Good values are also derived for methane and the LPGs. The worst relative performance is again derived for the two alcohols. The values derived for gravimetric and volumetric storage efficiency have to be evaluated with respect to the issue of storing and transporting the input species. Higher hydrocarbons, LPGs, and alcohols generally offer considerable advantages compared to species that have to be transported in cryogenic state in this respect.

**Table 14** Gravimetric and volumetric transport efficiency for investigated input species

	Gravimetric conversion efficiency	Volumetric conversion efficiency
	kg H <sub>2</sub> /kg fuel	liters H <sub>2</sub> /liter fuel
Methane	0.35	2.06
Propane	0.32	2.64
Butane	0.32	2.69
Heptane	0.31	3.00
Octane	0.31	3.08
Methanol	0.11	1.25
Ethanol	0.17	1.93

Carbon monoxide and hydrogen are oxidised into carbon dioxide and steam in the reduction cycle of the RESC. Some of this oxidation occurs within the SIR, where oxygen is drawn out of the contact mass. The remaining quantities of carbon monoxide and hydrogen are subsequently burned in the lean gas burner unit, which requires a supply with oxygen (or air in case of a terrestrial application, respectively). The amount of oxygen required by the lean gas burner unit is presented in the first column of Table 15. The amount of oxygen and input fuel required by the external burner unit – assuming that such a unit is installed – are presented in the columns two and three per mole of input gas.

**Table 15** Oxygen requirement for lean gas burner and input oxygen/fuel input gas streams for external burner unit

	O <sub>2</sub> required for lean gas burner	O <sub>2</sub> required for external burner	Fuel stream for external burner
	mol <sub>O<sub>2</sub></sub> /mol <sub>input</sub>	mol <sub>O<sub>2</sub></sub> /mol <sub>input</sub>	mol/mol <sub>input</sub>
Methane	0.62	0.19	0.10
Propane	1.48	0.16	0.03
Butane	1.92	0.23	0.04
Heptane	3.22	1.20	0.11
Octane	3.66	1.37	0.11
Methanol	0.61	0.00	0.00
Ethanol	1.02	0.07	0.02

Oxygen consumption per mole of hydrogen produced is presented in Table 16. A particularly small oxygen consumption is derived for LPGs, whereas methanol requires comparably large quantities of oxygen for the hydrogen production process.

**Table 16** Oxygen requirement per mole of hydrogen produced

	Without external burner	With external burner
	mol <sub>O<sub>2</sub></sub> /mol <sub>H<sub>2</sub></sub>	mol <sub>O<sub>2</sub></sub> /mol <sub>H<sub>2</sub></sub>
Methane	0.226	0.295
Propane	0.211	0.234
Butane	0.209	0.234
Heptane	0.207	0.284
Octane	0.207	0.285
Methanol	0.343	0.343
Ethanol	0.259	0.276

## 5.2 Thermal energy balance of the conversion process

The RESC thermal energy balance is presented in Table 17 for the investigated input species. The reduction cycle is generally exothermic, whereas the oxidation cycle is endothermic for all gases considered within this investigation. The overall thermal energy balance (i.e. one full reduction cycle followed by a full oxidation cycle) is slightly endothermic for all fuels except for methanol. Higher hydrocarbons as well as methane require the largest external thermal energy input. Values in excess of 30 kJ per mole of hydrogen produced are derived. The calculations are based on the “reference case” RESC with an operating temperature of 800°C, and a recycle rate of 50%. The subscript “input” refers to the stream of RESC input gases, whereas the subscript “H<sub>2</sub>” refers to the stream of hydrogen produced.

**Table 17** Compressed thermal energy balance for the investigated input gases

	Reduction cycle	Oxidation cycle	Overall	Heating requirement
	kJ/mole <sub>input</sub>	kJ/mole <sub>input</sub>	kJ/mole <sub>input</sub>	kJ/mole <sub>H<sub>2</sub></sub>
Methane	-64.20	148.14	83.94	30.49
Propane	-293.63	378.56	84.93	12.07
Butane	-372.98	493.33	120.35	13.13
Heptane	-306.10	836.92	530.82	34.13
Octane	-348.05	951.31	603.25	34.12
Methanol	-154.13	95.75	-58.39	-32.81
Ethanol	-170.54	212.77	42.23	10.68

### 5.3 Hydrocarbon to hydrogen conversion efficiency

The overall conversion efficiency  $\eta$  (in %) of the RESC process is defined according to equation E19. This definition considers the dimensionless number of moles of hydrogen ( $n$ ) produced out of each mole of hydrocarbon fuel supplied. Energy content of hydrogen and hydrocarbon fuels is compared with respect to the lower heating value (LHV).

$$\eta = 100 \frac{n \times LHV(H_2)}{LHV(Fuel)} \quad (E19)$$

The thermal energy balance of the RESC system is positive (for all species but methanol), i.e. the overall conversion process is endothermic. Thus, an additional source of heat is required to maintain the SIR operating temperature even with the assumption that there is no flux of heat to ambient.

Two cases are thus investigated:

- (a) RESC system with an external hydrocarbon burner
- (b) RESC system without an external hydrocarbon burner (process heat is available from another source)

Applying option (a), some of the hydrocarbon fuel is burned in an additional hydrocarbon burner unit to produce the thermal energy required to run the process. This results in a small system package that can operate independently without requiring an external heat source, at the cost of removing a fraction of the RESC input species plus oxygen out of the desired conversion process. Option (b) is particularly interesting if an external source of heat is available. This external heat source could be derived from solar energy (e.g. concentrated solar energy on the lunar surface) or waste heat from a nuclear power plant, for instance. Utilising an external energy source is beneficial with respect to the hydrocarbon to hydrogen conversion efficiency.

#### 5.3.1 Variation of the conversion efficiency with recycle rate and temperature

The plot shown on the left hand side of Figure 20 shows the variation of RESC process efficiency with methane as fuel as a function of recycle rate and process temperature. Applying very small recycle rates leads to low conversion efficiencies primarily due to the low concentrations of steam and carbon dioxide in the reformer input gas stream. Thus, only a fraction of the hydrocarbon fuel can actually be converted into hydrogen and carbon monoxide within the reformer, and only this small fraction can reduce iron oxides within the SIR. A limiting recycle rate is primarily derived with higher process temperatures. If a recycle rate is applied that is smaller than the limiting rate, the RESC process efficiency is drastically reduced down to almost zero. The recycle gas stream thus contains large volume fractions of methane fuel and only little quantities of carbon dioxide and steam that would be required with the reforming reaction. The process can thus not be operated appropriately, and large quantities of methane pass through the system without getting reformed, and thus also without reducing iron oxides. An external supply with steam or carbon dioxide would therefore be required if the process was to be operated with very small recycle rates or

without any recycling, respectively. Maximum efficiencies derived for the RESC process with methane fuel are in the order of 75%. Applying larger recycle rates is neither beneficial with respect to the overall conversion efficiency, nor with respect to the larger volumes that have to be circulated within the system. A process temperature level in the range of 800°C is sufficient to achieve good overall efficiencies. Applying higher temperatures does not lead to an increase in overall conversion efficiency due to the energy requirements of heating the gases up to process temperature. A reduction in temperature is particularly limiting with respect to the SIR performance.

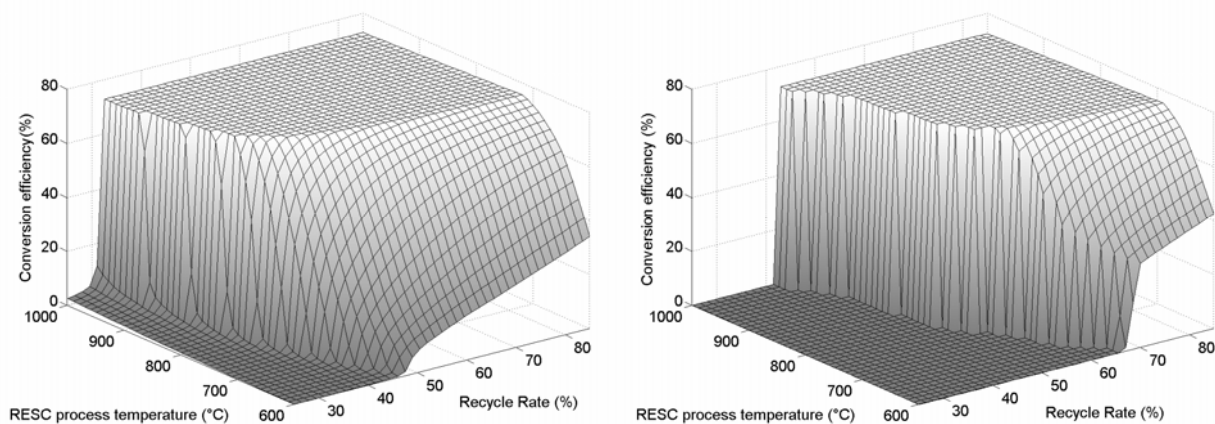


**Figure 20** Overall RESC conversion efficiency with methane (left) and heptane (right) input gas as a function of RESC process temperature and recycle rate (%)

Maximum conversion efficiencies achieved with heptane as input gas are in a similar range to the values calculated for methane as input gas. Conversion efficiencies derived for the two input gases are compared in Figure 20. Running the RESC on heptane fuel requires significantly higher recycle rates in order to achieve these high conversion efficiencies, though. A strong reduction in efficiencies is again derived if the recycle rate is smaller than the limiting recycle rate for the investigated temperature level.

### 5.3.2 Conversion efficiency for the investigated RESC input species

Input species to hydrogen conversion efficiencies are considered for a process temperature of 800°C and recycle rates between 40% and 60% in the following. Variation of the conversion efficiency for the case of an external hydrocarbon burner unit is presented in Figure 21. Peak values in the order of 65% to 85% are derived for the input species considered. A limiting recycle rate between 40% and 45% is derived for LPGs and higher hydrocarbons, with heptane and octane offering almost identical efficiencies. Alcohols and methane offer good conversion efficiencies even with small recycle rates. The conversion efficiency of methane matches that of ethanol over the complete range of conversion efficiencies investigated.

Slightly higher conversion efficiencies are derived for the case, that the process heat is not generated by a hydrocarbon burner unit, as presented in Figure 22. Maximum conversion efficiencies are generally in the order of 5-10% better than with a hydrocarbon burner unit. The relative performance of the species investigated matches the distribution already derived for the case of an external hydrocarbon burner unit; only methane offers a considerable better relative performance.

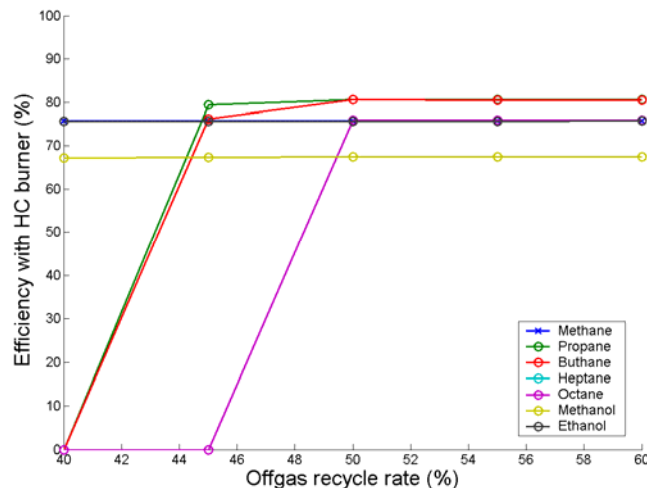


**Figure 21** Conversion efficiencies for different fuels with an external hydrocarbon burner unit

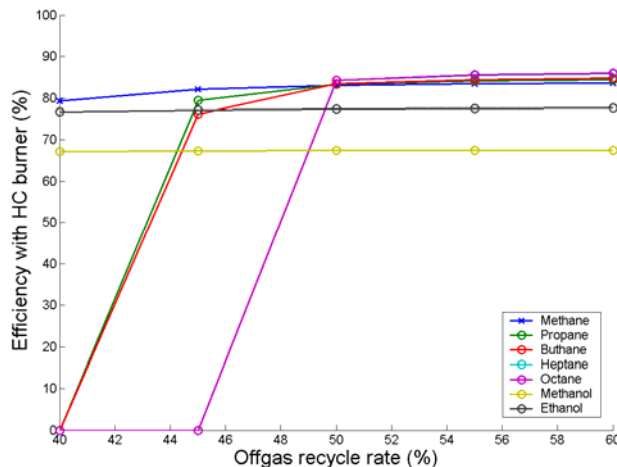


**Figure 22** Conversion efficiencies for different fuels without an external hydrocarbon burner unit

Peak hydrocarbon to hydrogen conversion efficiencies achieved with the different input species are presented in Table 18. Calculated efficiencies for methane, heptane, and octane versus LHV are almost identical. Significantly higher efficiencies are only derived for propane and butane fuel. LPG is therefore an interesting hydrocarbon source for hydrogen production with the RESC process. Conversion efficiencies derived for the two alcohols

considered are considerably lower than with the other input species investigated. This can be traced back to the particularly low carbon monoxide and hydrogen utilisation rates within the SIR.

**Table 18** Maximum conversion efficiencies computed for the RESC with different input species

	Efficiency with external burner	Efficiency without external burner
	(%)	(%)
<b>Methane</b>	74.8	84.0
<b>Propane</b>	79.8	84.9
<b>Butane</b>	79.7	85.3
<b>Heptane</b>	75.0	86.4
<b>Octane</b>	75.0	86.5
<b>Methanol</b>	67.6	67.6
<b>Ethanol</b>	74.8	77.9

#### 5.4 Evaluation of RESC system performance as a function of input gas

An evaluation of RESC input species was made in order to compile the individual species performance data computed with the envisaged application into a single performance indicator. Thus, a ranking of input species options for on-site hydrocarbon to hydrogen conversion is derived. This evaluation was made with respect to the following three evaluation categories:

**Transport and storage properties:** evaluation with respect to the gravimetric and volumetric energy storage density (energy per unit of mass and per unit of volume) as well as the boiling point (assuming that the boiling temperature indicates the relative difficulty of storing a species; a boiling temperature of  $-161.6$  for methane indicates a cryogenic storage, which is inevitably more challenging than storing higher hydrocarbons and alcohols, that are still in liquid state at temperatures in excess of 300K, for instance)

**RESC system dimensions:** evaluation of governing aspects of the RESC system dimensions, addressing the relative size of governing system components; the four aspects considered with this evaluation are the internal flow rate (methanol has e.g. twice the flow rate of heptane, requiring either a larger unit, or higher internal flow velocities), heat recuperation system of the reduction cycle (indicates how much thermal energy has to be transferred from off-gas to input species), overall thermal input (indicates the relative size of the external heat source), and lean gas oxygen consumption (indicates how much oxygen is consumed in combusting the lean gas)

**Input species to hydrogen conversion efficiencies:** evaluation of the overall conversion efficiencies of the different input species with and without considering an external hydrocarbon burner unit

Each of the properties was ranked with respect to the relative performance, assigning a score of one to the species with the best performance, and a score of seven to the species with the worst relative performance. Individual property scores were subsequently summed up, giving a overall input species option score. Small scores therefore indicate a good relative performance, large scores indicate a bad relative performance.

Results of the evaluation procedure are presented in Table 19 for the two cases with and without an external hydrocarbon burner unit. Detailed evaluation score tables are attached in Appendix B on pages 70 and 71.

**Table 19** Results of the RESC input species evaluation process

	Transport & storage properties	RESC system dimensions	Efficiency with external burner	Total score with external burner	Efficiency without external burner	Total score without external burner
<b>Methane</b>	14	20	6	40	5	39
<b>Propane</b>	12	15	1	28	4	31
<b>Butane</b>	11	13	2	26	3	27
<b>Heptane</b>	9	13	4	26	2	24
<b>Octane</b>	6	9	3	18	1	16
<b>Methanol</b>	18	22	7	47	7	47
<b>Ethanol</b>	14	20	5	39	6	40

Results indicate, that LPGs and higher hydrocarbons result in the best relative performance of the range of species considered within this initial investigation. These species offer a compact and lightweight transportation (high gravimetric and energetic energy density with an easy transport in liquid state) and can be efficiently utilised as feedstock for on-site hydrogen production procedures. Particularly the possibility to transport LPGs and higher hydrocarbons in simple storage vessels make these species an interesting option, considering the problems and limitations linked to storing and transporting cryogenic hydrogen over the course of weeks or months.

Alcohols did not receive good evaluation scores, although offering a very convenient transport in liquid phase. They offer the lowest gravimetric and volumetric energy density out of all the species considered. The computed hydrocarbon to hydrogen conversion efficiencies are also very low.

The evaluation process therefore suggests a further consideration of higher hydrocarbons as feedstock for on-site hydrogen production. These species combine good transport properties with high conversion efficiencies and a low lean gas burner oxygen consumption.

## 5.5 Investigations of the combined RESC/fuel cell system

Conversion of a hydrocarbon fuel into electric energy is enabled by utilising a RESC system in combination with a fuel cell module. Two fundamental approaches in designing this combined system suggest themselves: firstly, operation of a low- or high-temperature fuel cell module drawing fuel out of a storage vessel that is supplied with pure hydrogen produced by the RESC system. Secondly, the direct combination of RESC and a high-temperature fuel cell within a common thermal enclosure. Both approaches offer characteristics that suggest their utilisation with specific applications. A thermodynamic analysis of both approaches in combined system design is presented in the following.

### 5.5.1 RESC/fuel cell system with intermediate storage

The first approach in RESC/fuel cell power system design is to apply intermediate gas storage vessels for storing the hydrogen output gas produced by the RESC system. The gas could thus be drawn from the storage vessels on demand, which in turn would allow to operate the fuel cell unit according to required output power profiles and not with respect to the RESC hydrogen production output. Operation without a common system temperature (i.e. RESC and fuel cell are not operated with the same temperature, other than with a direct combination system) also enables the utilisation of low-temperature fuel cells (PEMFC) in stationary and/or mobile applications because no common thermal enclosure and management system is required. High-temperature fuel cells are nevertheless investigated in the following analysis of the two approaches in combined RESC/fuel cell system design. The reason for considering only a high-temperature fuel cell even with the intermediate storage approach, that could just as well be operated with a low-temperature fuel cell, was to provide a direct comparison between the two approaches in combined system design with the identical fuel cell performance. The fuel cell performance is therefore not responsible for the considerable differences in operation and efficiency of the two systems; the difference in the overall system conversion efficiency is directly linked to the different operating principles applied with two approaches in combining the RESC and the fuel cell unit, only.

#### Advantages of the intermediate RESC product gas storage approach

- Power generation can be actively controlled according to output power requirements, rather than by the availability of RESC product gas
- Intermediate storage of hydrogen enables the supply of a number of different stationary and mobile applications with hydrogen gas from one common RESC hydrogen production plant
- A simple system design can be applied, where the fuel cell is installed independently of the hydrogen production system; this is particularly interesting with mobile applications, where the onboard power system could thus be loaded with hydrogen from a stationary production system

### Limitations of the intermediate RESC product gas storage approach

- Fuel cell product water has to be collected and stored with the fuel cell power system. This water has to be re-supplied to the RESC system in order to enable a closed-loop operation. Water condensation, storage, and waste heat rejection are challenging issues particularly with low-temperature fuel cell systems, where condensation and heat rejection has to be made at temperatures below 100°C
- RESC output gas storage equipment has to be installed (product gas management, compression/liquefaction, and a gas storage utility)
- Steam required with RESC operation in oxidation mode has to be generated from a reservoir of (liquid) water; this adds a considerable share to the overall thermal energy requirements of the system

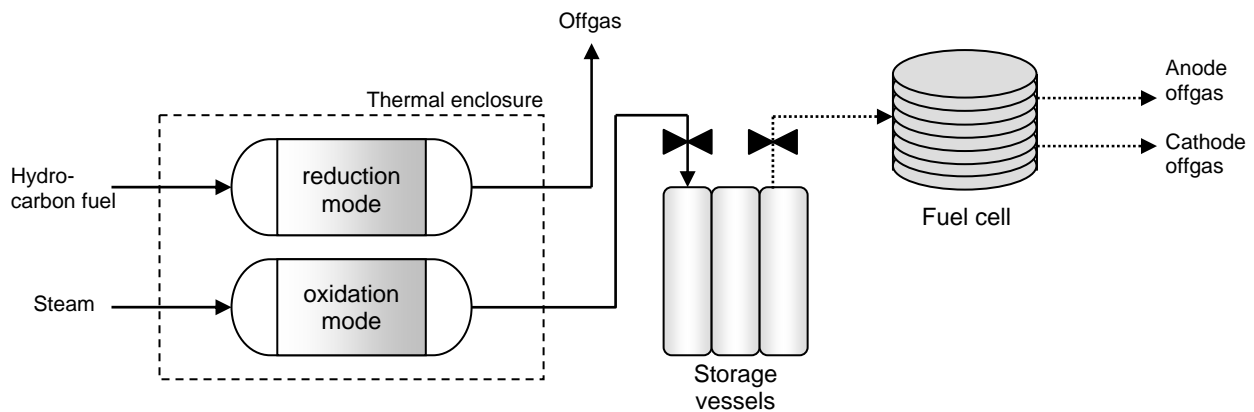


**Figure 23** RESC/fuel cell system with intermediate RESC product gas storage

Straight-forward mass and energy balances of the SOFC reference fuel cell module considered with the combined system calculations are presented in Table 20.

**Table 20** Energy balance of the reference fuel cell module

Property	Value	Unit
LHV	242	kJ/mole
Electric energy	144.8	kJ/mole
Efficiency (vs. LHV)	59.8	%
Efficiency (@85% FU)	50.9	%

The hydrogen fuel to electric conversion efficiency is estimated as 59.8% (available electric energy versus LHV of fuel). This figure is derived by considering a single cell voltage of 0.75V (which is a typical cell voltage for a current density of 350 mA/cm<sup>2</sup> applied e.g. in [34] for describing regular operation of a SOFC), and comparing the electric energy production per mole of hydrogen with the LHV. This produces a theoretical efficiency of 59.8%. This value has to be multiplied with the fuel utilisation rate (FU), which describes the fraction of

fuel that is effectively utilised with the desired electrochemical conversion process. A typical value of FU for SOFCs is in the order of 85%, again following calculations presented in [34]. The net conversion efficiency (input energy of fuel versus electrical output energy) of the SOFC module is thus estimated as being 50.9%.

Calculation of the overall conversion efficiency of a RESC/fuel cell system (i.e. input energy of the hydrocarbon fuel into electrical energy) can be broken down into two separate calculations: firstly, the calculation of input species into pure hydrogen; and secondly the conversion of hydrogen into electric energy.

Results of thermodynamic calculations of the first conversion process have already been presented with chapter 5. The reader is referred to Table 18 for a compiled overview of input species to hydrogen conversion efficiencies.

A compressed overview of the overall fuel to electric conversion efficiency is presented in Table 21 for all of the seven potential RESC input species considered within this initial investigation.

**Table 21** Overview of hydrocarbon fuel to electric conversion efficiencies for the seven investigated RESC input species

	Efficiency with external HC-burner		Efficiency without external HC-burner	
	Input species to hydrogen	Hydro-carbon to electric	Input species to hydrogen	Hydro-carbon to electric
	(%)	(%)	(%)	(%)
Methane	74.8	38.1	84.0	42.7
Propane	79.8	40.6	84.9	43.2
Butane	79.7	40.5	85.3	43.4
Heptane	75.0	38.2	86.4	44.0
Octane	75.0	38.2	86.5	44.0
Methanol	67.6	34.4	67.6	34.4
Ethanol	74.8	38.1	77.9	39.6

Overall conversion efficiencies are thus in the order of 34 to 44%, depending on input species, and if an external hydrocarbon burner is applied with the RESC or if an external heat source is available.

### 5.5.2 Direct combination of RESC and high-temperature SOFC

This approach in combined system design is based on a RESC system (consisting of at least one SIR in oxidation mode and one SIR in reduction mode operated in parallel) continuously supplying a high-temperature fuel cell system with hydrogen. In case of the direct combination approach, the RESC output gas is not cooled down and stored prior to

utilisation. Possibilities and limitations of this approach in combined system design are compiled below:

### Advantages

- Direct conversion of hydrocarbon fuel into electricity
- Efficient conversion of hydrocarbons into hydrogen
- Feedback of fuel cell anode offgas into the oxidation mode SIR
- Good performance of the SOFC with hydrogen as fuel
- RESC and fuel cell are operated with the same system temperature; thus, only one thermal enclosure has to be installed with the system
- Intermediate cooling/condensation of SOFC output gases for product water recovery is not required; this aspect considerably simplifies the overall system design and reduces the thermal energy requirements in the oxidation cycle
- Operation of such a system is particularly beneficial with a system supplying a constant electrical (base) load without transients

### Limitations

- Utilisation primarily for base-load conditions where no transient operation of the fuel cell is required; load-following operation is strongly limited by the thermal characteristics of the overall system
- Storage of hydrogen is not enabled; a supply of disseminated applications with RESC product gas would have to be considered with a separate installation of a product gas storage system following the intermediate RESC product gas storage design approach

A schematic of the direct combination RESC/SOFC system is presented in Figure 27. The direct feed of oxidation cycle SIR product gases into the fuel cell module is highlighted. The SOFC anode output gas feedback loop is shown a dotted line, suggesting that this setup is possible, but not necessarily the only solution applicable with a re-feeding of product water.

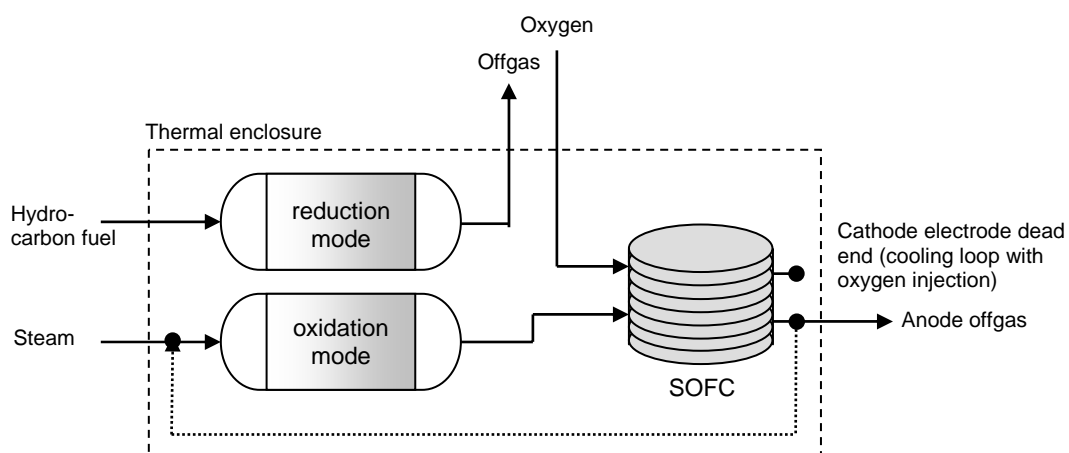


**Figure 24** Schematic of the direct combination RESC/SOFC system

### 5.5.3 Thermodynamic investigation of the direct RESC/SOFC combination

A thermodynamic analysis of the combined RESC/SOFC system has been made with the component models developed within the research project. The full RESC system with reduction and subsequent oxidation cycle were thus considered with a SOFC operating directly with the hydrogen/steam product gas mixture coming from the oxidation cycle SIR. The following assumptions were applied in computing the thermodynamic analysis of the combined system:

- Standard consideration of the RESC in reduction cycle with an off-gas temperature of 150°C, species input temperatures of 25°C, and different hydrocarbon input species
- Input water required with the oxidation cycle does not have to be vaporised (steam coming directly from the SOFC anode outlet is utilised as input species)
- Input gas in oxidation cycle is not pure steam, but a steam/hydrogen mixture (the gas contains some 15% of hydrogen, assuming a fuel utilisation of 85% in the fuel cell module); this feed of hydrogen reduces the utilisation of steam with the oxidation of contact mass, but is acceptable with respect to the equilibrium gas concentrations
- No heat recuperation system is applied with the RESC oxidation cycle (outlet gases are directly fed into the SOFC without cooling them down)
- A common system temperature of 800°C is applied with RESC and fuel cell module
- A SIR output gas recycle rate of 50% is applied with the calculations
- A fuel utilisation rate of 85% is assumed with the SOFC
- The SOFC is assumed to be operated with 0.75V and 300 mA/cm<sup>2</sup>

The feedback loop of fuel cell output gas into the SIR in oxidation mode is one of the key advantages of the direct combination system. Assuming a fuel utilisation of 85% within the fuel cell module, the anode off-gas still contains some 15% of hydrogen. This 85%/15% steam/hydrogen mixture is able to oxidise Wuestite into Magnetite, and thus to achieve a full conversion of the contact mass. The limiting value would be a 40.9% hydrogen content with a temperature of 800°C, for instance. In this case, the input gas in oxidation would not be able to achieve a conversion of Wuestite into Magnetite. The fuel cell unit has therefore always got to be operated with a high fuel utilisation rate in order to achieve a sufficient oxidation potential within the SIR. Effective and equilibrium concentrations are investigated for a case of 800°C with the Baur-Glaessner diagram presented in Figure 25.

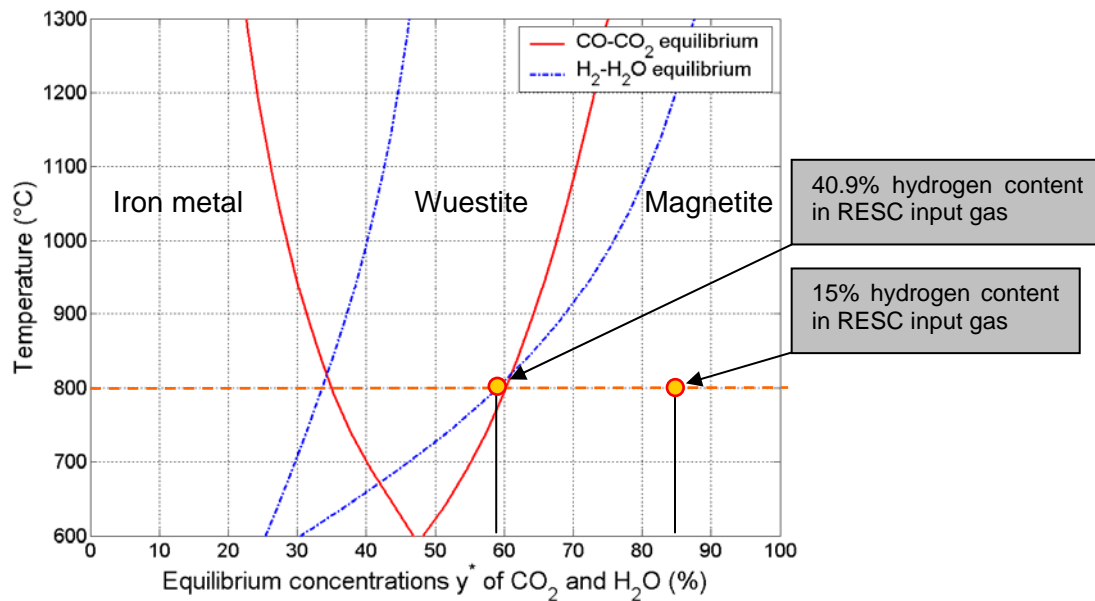


**Figure 25** Comparison of effective and required oxidation cycle input gas hydrogen content to achieve a full conversion into Magnetite at 800°C

A detailed analysis of the overall system energy balance is presented with methane, heptane, and methanol input species in the following. These three species are considered because they represent the favoured ISRU fuel (methane), a liquid higher hydrocarbon (heptane), and a liquid alcohol (methanol). A straight-forward comparison between each of these three types of species is enabled. Performance figures derived for other species of the same category (e.g. octane versus heptane or ethanol versus methanol) are within similar ranges, and are therefore not written explicitly with the discussion presented below.

**Table 22** Energy balance for the RESC reduction cycle

Reduction cycle	Methane fuel		Heptane fuel		Methanol	
	Temperature (°C)	Heat balance (kJ/mole)	Temperature (°C)	Heat balance (kJ/mole)	Temperature (°C)	Heat balance (kJ/mole)
Hydrocarbon feed	25	0	25	0	25	0
Evaporator	-	0	150	61	150	43
Gas mixing	567	0	587	0	561	0
Heat exchanger	800	44	800	209	800	49
Reformer	800	235	800	1261	800	105
SIR	800	36	800	129	800	23
Offgas treatment	150	-387	150	-2010	150	-383
<b>Energy balance I</b>	-	<b>-72</b>	-	<b>-350</b>	-	<b>-163</b>

The RESC energy balance for reduction cycle is presented in Table 22. The thermal energy balance of all three investigated species is negative, following the governing principles presented with chapter 5.

The RESC oxidation cycle energy balance is also negative with all three investigated species, according to the figures presented in Table 23. Due to the fact that a hot steam/hydrogen is fed into the SIR, no energy is required for evaporating water and heating it up to process temperature. Heat recuperation is not possible because the off-gas is directly fed into the fuel cell at system temperature. This leaves the exothermic sponge iron reaction as only thermal energy source, generating between 43 kJ and 380 kJ per mole of input gas supplied to the system. Reduction and oxidation cycle of the RESC are therefore exothermic with the combined RESC/fuel cell system. Unlike with the pure hydrogen production cycle, no external heat source is therefore required to operate the system, but considerable quantities of excess waste heat is generated with the conversion process.

**Table 23** Energy balance for the RESC oxidation cycle

Oxidation cycle	Methane fuel		Heptane fuel		Methanol	
	Temperature (°C)	Heat balance (kJ/mole)	Temperature (°C)	Heat balance (kJ/mole)	Temperature (°C)	Heat balance (kJ/mole)
Feed	800	-	800	-	800	-
Evaporator	800	-	800	-	800	-
Heat exchanger	800	-	800	-	800	-
SIR	800	-67	800	-380	800	-43
Offgas treatment	800	-	800	-	800	-
<b>Energy balance II</b>	-	<b>-67</b>	-	<b>-380</b>	-	<b>-43</b>

Hot RESC output gas of the oxidation cycle is fed into the SOFC unit, and thus directly utilised for electric power generation purposes with the direct combination design. Net electrical output power generation per mole of input gas is presented in Table 24 for each of the three investigated species along with the overall system waste heat production (RESC and fuel cell). Derivation of the electrical energy does not consider the 75% fuel utilisation rate due to the fact that hydrogen that is not consumed in the cell is re-supplied after feeding the gas through the SIR. Hydrogen in the fuel cell offgas is thus not lost for the desired conversion process. This contributes to the good overall conversion efficiency calculated for the direct combination design.

The overall thermal energy balance is exothermic with the conversion process of hydrocarbon fuel into electrical output power due to waste heat production within the fuel cell unit. The case of a RESC system with an additional hydrocarbon burner unit is nevertheless included in the following analysis in order to provide a straight-forward comparison with the previously considered RESC system options.

**Table 24** Energy balance for the fuel cell unit

<b>Fuel cell</b>						
	<b>Methane fuel</b>		<b>Heptane fuel</b>		<b>Methanol</b>	
	Property	Unit	Property	Unit	Property	Unit
LHV input species	802	kJ/mol	4464	kJ/mol	638	kJ/mol
<b>Without hydrocarbon burner</b>						
Mol H <sub>2</sub> /mol fuel	2.8	mol/mol	15.6	mol/mol	1.8	mol/mol
Electrical energy	398	kJ/mol	2251	kJ/mol	258	kJ/mol
Waste heat	404	kJ/mol	2213	kJ/mol	380	kJ/mol
<b>With hydrocarbon burner</b>						
Mol H <sub>2</sub> /mol fuel	2.5	mol/mol	14.0	mol/mol	1.8	mol/mol
Electrical energy	362	kJ/mol	2028	kJ/mol	258	kJ/mol
Waste heat	440	kJ/mol	2436	kJ/mol	380	kJ/mol

The overall efficiency of the conversion process (i.e. chemical energy of the fuel into electrical output power) is presented in Table 25. Net conversion efficiencies in the order of 40 to 50% are derived for all three types of RESC input gas.

**Table 25** Energy balance for the hydrocarbon to electric conversion process

<b>Overall energy balance</b>						
	<b>Methane fuel</b>		<b>Heptane fuel</b>		<b>Methanol</b>	
	Property	Unit	Property	Unit	Property	Unit
Fuel to electrical efficiency without hydrocarbon burner	49.6	%	50.4	%	40.4	%
Fuel to electrical efficiency with hydrocarbon burner	45.1	%	45.4	%	40.4	%

## 5.6 Compilation of key results derived with the RESC system simulations

- The overall hydrocarbon to hydrogen conversion process of all input species but methanol is endothermic even with the simplified thermodynamic analysis applied within this study; an additional heat source therefore has to be considered with the RESC system
- Availability of an external heat source (e.g. solar energy, heat of a nuclear reactor) results in an average increase in hydrocarbon to hydrogen conversion efficiency in the order of 5-10% relative to the performance with a system where the heat is provided by combusting a fraction of input fuel in a burner unit
- Hydrocarbon to hydrogen conversion efficiencies are in the order of 67-85%, depending on process parameters and input species
- The two governing properties in RESC operation (system temperature and SIR offgas recycle rate) provide a characteristic operating behaviour, prohibiting operation with low temperatures and small recycle rates, and providing an almost constant system performance once a limiting recycle rate is exceeded with system temperatures in excess of 700°C
- Higher hydrocarbons and LPGs showed the best overall performance with the RESC input species evaluation, providing compact and lightweight transportation, and high hydrocarbon to hydrogen conversion efficiencies
- Alcohols received the lowest scores of all RESC input species investigated, due to their low gravimetric and volumetric energy densities, as well as their low hydrocarbon to hydrogen conversion efficiencies
- The direct combination of RESC and SOFC results in a considerably more efficient operation of the system (e.g. for methane: 45.1/49.6% for direct combination with/without a hydrocarbon burner versus 38.1/42.7% for intermediate storage with/without a hydrocarbon burner) than a system with RESC product gas intermediate storage
- Fuel cell waste heat – available at elevated temperatures with the SOFC considered with the direct combination RESC/fuel cell system – can be efficiently utilised for providing heat to the endothermic hydrocarbon to hydrogen conversion process

## 6 Applying the SIR for oxygen extraction from Lunar regolith

Oxygen can be extracted from surface materials readily available on Moon and Mars if the regolith is exposed to a reducing atmosphere at elevated temperatures. Thus, hydrogen brought from the Earth could be converted into steam, releasing the oxygen after decomposition.

A simplified schematic of the investigated oxygen extraction principle is shown in Figure 26. Hydrogen (brought from the Earth and/or produced by decomposing water already produced with the system) is supplied to the system. Carbon monoxide could also be applied for contact mass reduction. This would be particularly relevant if the contact mass reduction is achieved by feeding a synthesis gas produced from hydrocarbons supplied from Earth and containing hydrogen as well as carbon monoxide into the reactor. The input gas is heated up to process temperature, and is applied to reduce the oxidised regolith material within the reactor. A fixed bed reactor is utilised with the standard SIR system utilised with the demonstration prototype operated at Graz University of Technology. A fluidised bed reactor would probably be applied with a system operated with lunar regolith. This reactor design approach would simplify handling and operation of the system with solid input material composed of smaller particles and dust, rather than the porous contact mass pellets utilised with the SIR. Thermodynamic limits calculated in the following are applicable to either approach in reactor design, though.

A waste heat recuperation system is considered to draw heat out of the hot SIR offgases, and to transfer this thermal energy into the stream of input gas. Water separation is performed to remove the steam before re-feeding the hydrogen that was not utilised in the previous SIR cycle.

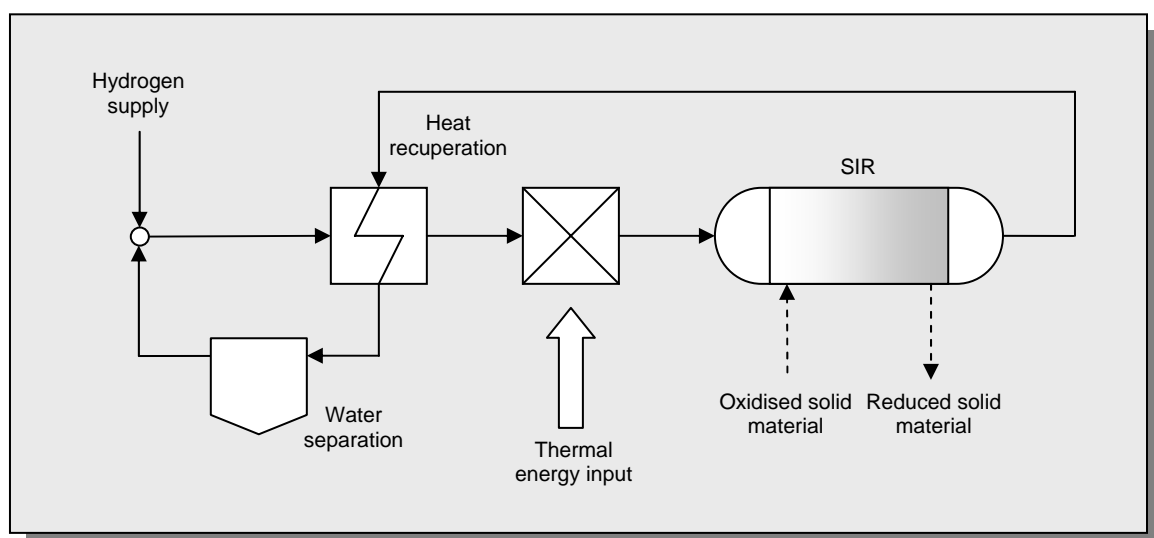


**Figure 26** Simplified schematic of the SIR plant layout for oxygen extraction

According to the principles presented within the previous chapters, oxygen can be drawn out of the contact mass as long as the equilibrium conditions between hydrogen and steam, as well as between carbon monoxide and carbon dioxide, are not fully achieved. This process is presented in Figure 27 for hydrogen and carbon monoxide, assuming that no steam and no carbon dioxide are fed into the reactor.

Carbon monoxide conversion is shown as shift from point I. (100% carbon monoxide, no carbon dioxide input gas) to point II. (carbon monoxide and carbon dioxide are in full equilibrium with the wuestite/magnetite phase). Hydrogen conversion is shown as shift between point III. (100% hydrogen, no steam in input gas feed) to point IV. (steam and hydrogen are in full equilibrium with the wuestite/magnetite phase).

Reduction of regolith material with carbon monoxide would theoretically be a feasible approach, but has not been considered with previous studies on Lunar oxygen production due to the superior performance of hydrogen in rocket propulsion.

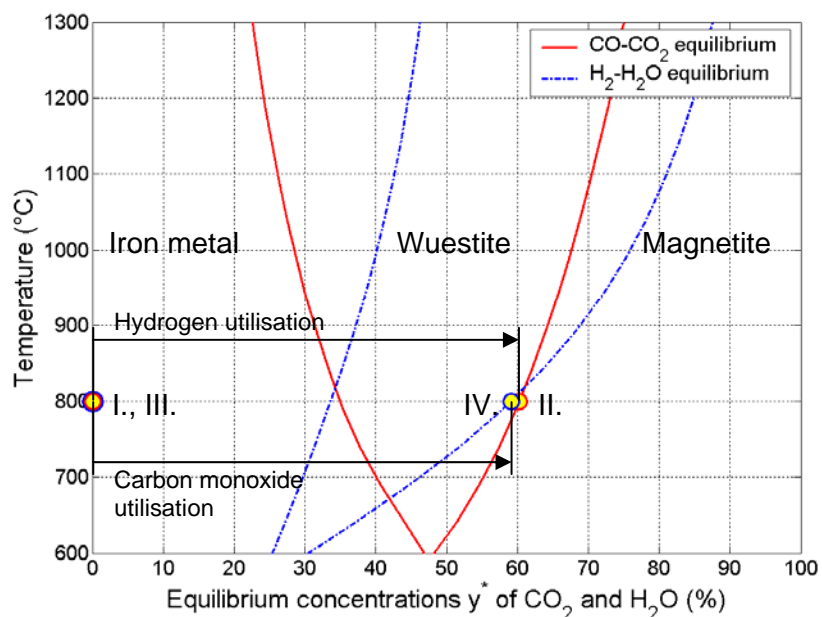


**Figure 27** Hydrogen to steam and carbon monoxide to carbon dioxide conversion with the sponge iron reaction

The fraction of hydrogen involved in reducing the contact mass is shown in Figure 28 as a function of SIR operating temperature. Elevated SIR operating temperatures therefore result in a compact system with high rates of hydrogen utilisation. Low temperatures result in high volumetric flow rates due to the low rates of hydrogen utilisation. This aspect has a strong influence on the overall thermal energy balance of the system, because hydrogen that is not utilised directly within the SIR has to undergo the complete thermal cycling required for the water separation process. High flow rates therefore also result in additional waste heat production that necessarily reduces the overall system efficiency.

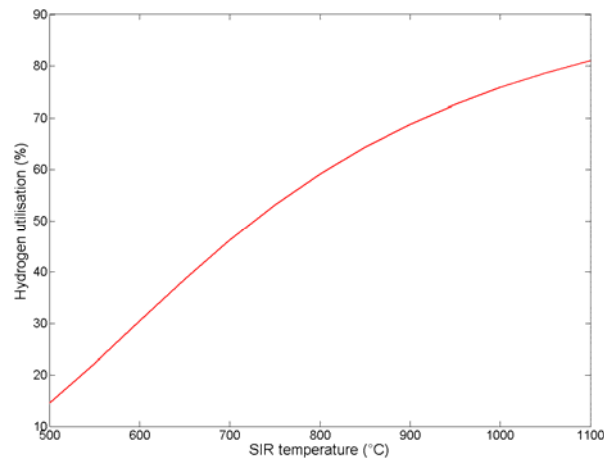


**Figure 28** Hydrogen utilisation as a function of SIR operating temperature

The overall thermal energy balance of the oxygen extraction system is presented in Figure 29. The following aspects were considered in deriving the figure:

- Heating up the hydrogen input gas and the solid input material (Magnetite) to SIR operating temperature
- Thermal energy balance of the SIR (i.e. the heat flux required to keep the SIR operating temperature constant as the reduction of solid material proceeds)
- Heat recuperation applied to cool the SIR offgas down to a temperature of 100°C
- Input gas (hydrogen) is assumed to be provided to the system at an average temperature of 300 K
- Solid input material (regolith) is assumed to be provided to the system at an average temperature of 0°C; solid material is assumed to be cooled down to 200°C before leaving the system
- Solid material is assumed to be pure Magnetite; including other (inactive) minerals into the Regolith composition would correspondingly increase the heating requirements
- Water condensation and cooling the SIR offgases below 100°C is not considered with the initial process energy balance

Calculations revealed, that the process is endothermic if the model assumptions outlined above are utilised. A net heat supply in the order of 40 kJ is required per mole of hydrogen utilised with the conversion process (i.e. per mole of water produced within the reactor). Detailed system analysis would have to be performed in order to determine the actual performance of an oxygen extraction system, considering realistic figures for heating requirements and heat recuperation system with solid and gaseous species as well as with Regolith instead of pure Magnetite. The simplified thermodynamic analysis therefore does not provide the level of insight required with a thorough analysis of the process.

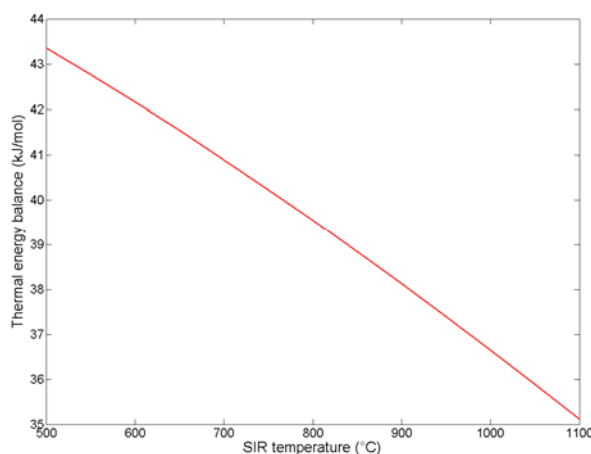


**Figure 29** Thermal energy balance as a function of SIR temperature

## 7 Hydrogen production with carbon monoxide as SIR reducing agent

Utilising a SIR system, hydrogen could theoretically be produced with carbon monoxide as SIR reducing agent. Carbon monoxide is a very interesting option in ISRU because it can be produced from carbon dioxide available in the Martian atmosphere without requiring a transport of species from Earth, as it would be the case with systems based on hydrogen or hydrocarbons, respectively. Carbon monoxide is also produced as by-product with the Sabatier reaction based ISRU plant suggested with the NASA Mars Reference Mission [24]. The Reference Mission ISRU plant schematic suggests to vent carbon monoxide - produced as by-product within the combined Sabatier/Reverse Water Gas Shift reaction - into the atmosphere. A utilisation of this carbon monoxide would therefore provide an additional hydrogen production capacity (producing hydrogen from steam within the SIR rather than with electrolysis) even with the base case Sabatier ISRU system.

The basic principle would be to feed carbon monoxide into the SIR in reduction mode, thus converting a fraction of the carbon monoxide supplied into carbon dioxide. This reaction would proceed until the equilibrium condition (equilibrium between carbon monoxide and carbon dioxide with the oxidation stage of the contact mass) is achieved. This implies, that only a certain fraction of the carbon monoxide supplied to the reactor could actually be utilised with the reduction of solid contact mass. SIR offgas would therefore contain a certain amount of carbon monoxide that cannot be utilised with the reduction of contact mass. This fraction of unused carbon monoxide feed can be calculated as a function of the reactor operating temperature by applying basic thermodynamic considerations.

If the SIR is subsequently switched into oxidation mode and steam is fed into the reactor, the contact mass would be re-oxidised and hydrogen would be produced. The second step in carbon monoxide to hydrogen conversion thus follows the fundamental process of the oxidation mode already discussed with the RESC system.

The basic principle of this operation is presented in Figure 31. Carbon monoxide utilisation is shown as shift in gas concentrations from point I (100% carbon monoxide) to point II (carbon monoxide and carbon dioxide are in full equilibrium with the wuestite/magnetite phase of the contact mass). Steam utilisation is shown as shift in gas phase concentrations between the conditions in point III (100% steam) to point IV (steam and hydrogen are in full equilibrium with the iron metal/wuestite phase of the contact mass). A simplified schematic of the carbon monoxide to hydrogen conversion process is shown in Figure 30.

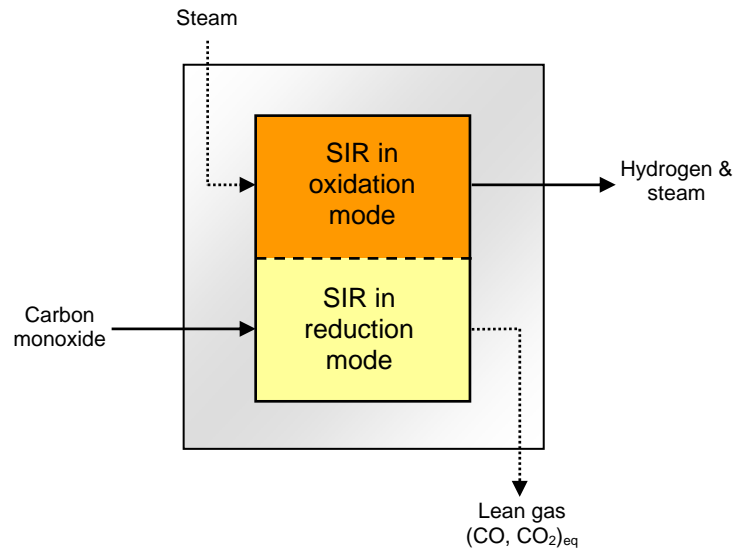


**Figure 30** Input and output species of the SIR applied in carbon monoxide to hydrogen conversion

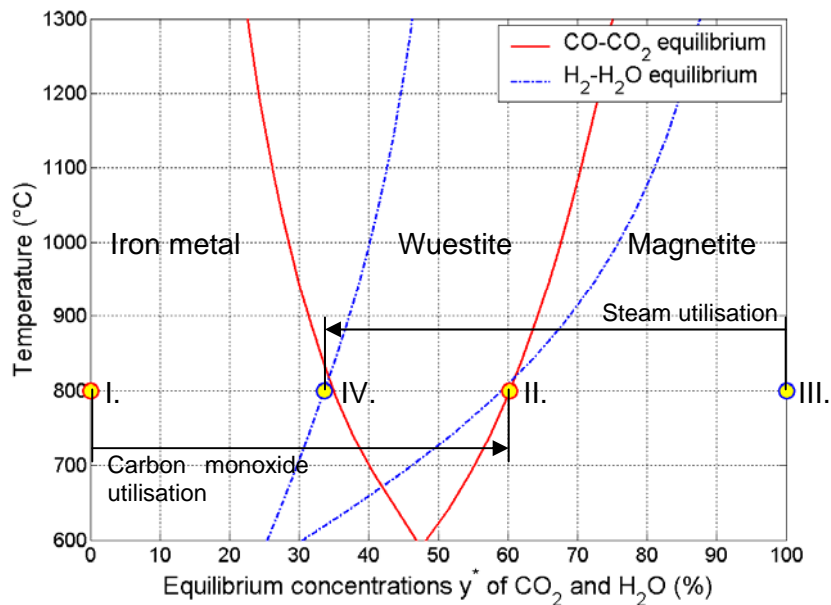


**Figure 31** Hydrogen production with carbon monoxide as SIR reducing agent

The governing parameter in this conversion process is the fraction of carbon monoxide utilised with the conversion process, i.e. the fraction of carbon monoxide that is participating in the reduction of iron oxides.

Carbon monoxide utilisation is presented as a function of SIR operating temperature in Figure 32. Utilisation rates in the order of 50% are derived for low operating temperatures. Higher utilisation rates are only derived for elevated operating temperatures, offering utilisation rates in excess of 70% with temperatures of 950°C and above.

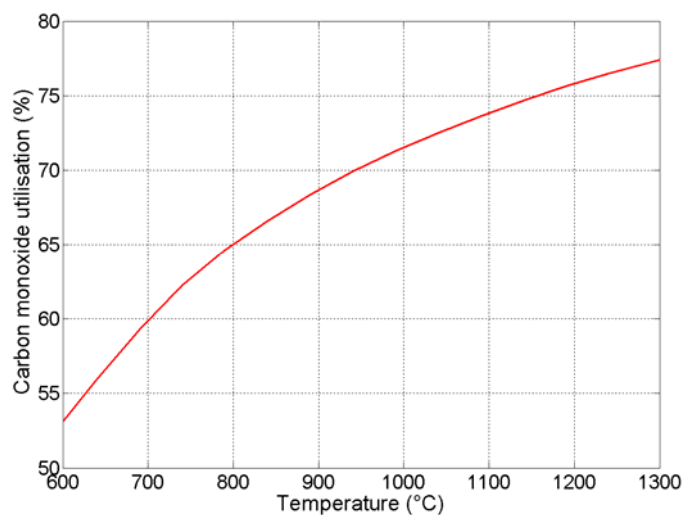


**Figure 32** Carbon monoxide utilisation as a function of SIR operating temperature

A considerable fraction of the total amount of carbon monoxide supplied to the SIR is thus lost for the conversion process into hydrogen. Remaining quantities of carbon monoxide leaving the reactor with the lean gas would have to be either separated from the carbon monoxide, or utilised in a burner unit (required to maintain the SIR at operating temperature) or in a high-temperature fuel cell unit, for instance. The low overall carbon monoxide to hydrogen conversion efficiency is not in favour of a wider utilisation of the process, though.

## 8 Applying the SIR for energy storage purposes

The SIR principle could also be applied to store energy. The term ‘Energy storage’ refers - in this particular context - to the possibility of utilising the contact mass in reduced state as means of providing an on-demand hydrogen production capacity. The contact mass (e.g. stored in cartridges) could be reduced with synthesis gas or carbon monoxide in a stationary ISRU plant in a first step. These cartridges could be sealed and easily stored over longer periods of times. When hydrogen fuel is to be drawn out of such a cartridge, the reduced contact mass would just have to be heated and supplied with steam to release a mixture of hydrogen and steam.

This storage system is not only applicable with stationary systems (e.g. hydrogen supply for an emergency fuel cell power unit), but also with mobile applications. The moderate mass-specific hydrogen storage capacity of pure iron strongly limits the range of applications, and seems almost prohibitive with a contact mass containing large fractions of minerals that do not participate in the REDOX cycles.

The mass-specific hydrogen storage capacity can be derived by dividing the hydrogen production capacity through the iron storage mass (e.g. how many kilograms of hydrogen can be theoretically produced if steam is supplied to an iron metal contact mass that is fully re-oxidised to the oxidation stage xxx). Theoretical values obtained for the case of a pure iron metal contact mass are presented below. The values given in Table 26 refer to the mass of pure iron metal and pure iron oxide, respectively. The mass of water (required for hydrogen production) and the mass of hydrocarbons or synthesis gas (required for contact mass reduction) are not included with the derivation of these figures.

**Table 26** Theoretical hydrogen storage capacity as a function of final iron oxide stage

		Hydrogen mass fraction <sup>1</sup>
FeO	Wuestite	3.6 wt% / 2.8 wt%
Fe <sub>3</sub> O <sub>4</sub>	Magnetite	4.8 wt% / 3.5 wt%
Fe <sub>2</sub> O <sub>3</sub>	Haematite	5.4 wt% / 3.8 wt% <sup>2</sup>

<sup>1</sup> wt% with respect to iron metal / wt% with respect to iron oxide investigated

<sup>2</sup> theoretical value, cannot be achieved with synthesis gas

The theoretical values presented have to be corrected if the contact mass is not pure iron metal, but rather a mixture of different minerals. Utilising Lunar or Martin regolith with an iron content in the order of 10-30% would therefore reduce the effective hydrogen storage capacity considerably. Net storage values in the order of 1 wt% are realistic, neglecting the mass of storage vessel and thermal management system required to achieve the process temperature.

## List of Abbreviations

APXS	Alpha particle x-ray spectrometer
FU	fuel utilisation
HEX	heat exchanger
HHV	higher heating value
ISRU	in-situ resource utilisation
LH2	liquid hydrogen
LHV	lower heating value
LOX	liquid oxygen
LPG(s)	liquid petroleum gas(es)
MB	Mössbauer spectrometer
Mini-TES	miniature thermal emission spectrometer
MER	Mars exploration rover(s)
MPF	Mars pathfinder
PEM(FC)	polymer electrolyte membrane (fuel cell)
RESC	reformer sponge iron cycle
RWGS	reverse water gas shift reaction
SIR	sponge iron reaction
SOFC	solid oxide fuel cell
VL1	Viking 1 lander

## List of figures

Figure 1 Governing parameters in RESC operation.....	6
Figure 2 Simplified schematic of the SIR.....	7
Figure 3 Simplified schematic of the RESC.....	8
Figure 4 RESC test rig installed at Graz University of Technology .....	9
Figure 5 Oxygen yield (mass of oxygen per mass of starting material) for 14 lunar soils and one lunar volcanic glass reacted at 1050°C.....	11
Figure 6 Regional distribution of iron oxide concentrations on the Moon.....	12
Figure 7 Lunar oxygen production plant.....	12
Figure 8 Data from Opportunity's Mini-TES plotted over a Pancam image of the Meridiani Planum landing site.....	15
Figure 9 Mössbauer spectrum showing minerals detected in a rock called "Clovis" in the "Columbia Hills" .....	15
Figure 10 Basic ISRU system for production of propellants and consumables.....	16
Figure 11 Example output plot of the reformer model; input gas composition: one mole CH <sub>4</sub> , one mole of CO <sub>2</sub> , and one mole of H <sub>2</sub> O .....	22
Figure 12 Example output plot of the reformer model; input gas composition: one mole of C <sub>7</sub> H <sub>16</sub> , five moles of CO <sub>2</sub> , and five moles of H <sub>2</sub> O.....	22
Figure 13 Baur-Glaessner diagram .....	24
Figure 14 Schematic of the RESC process in reduction mode .....	26
Figure 15 Schematic of the RESC process in oxidation mode.....	27
Figure 16 Moles of hydrogen produced per mole of methane and heptane supplied to the system.....	33
Figure 17 Fraction of total methane and heptane consumption required for heating purposes .....	34
Figure 18 Molar flux supplied to the SIR in case of methane and heptane fuel .....	34
Figure 19 Fraction of carbon monoxide and hydrogen supplied to the SIR that is utilised for iron oxide reduction in case of methane and heptane input gas .....	35
Figure 20 Overall RESC conversion efficiency with methane and heptane input gas as a function of RESC process temperature and recycle rate .....	40
Figure 21 Conversion efficiencies for different fuels with an external hydrocarbon burner unit .....	41
Figure 22 Conversion efficiencies for different fuels without an external hydrocarbon burner unit .....	41
Figure 23 RESC/fuel cell system with intermediate RESC product gas storage.....	46
Figure 24 Schematic of the direct combination RESC/SOFC system.....	48

Figure 25 Comparison of effective and required oxidation cycle input gas hydrogen content to achieve a full conversion into Magnetite at 800°C .....	50
Figure 26 Simplified schematic of the SIR plant layout for oxygen extraction.....	54
Figure 27 Hydrogen to steam and carbon monoxide to carbon dioxide conversion with the sponge iron reaction.....	55
Figure 28 Hydrogen utilisation as a function of SIR operating temperature .....	56
Figure 29 Thermal energy balance as a function of SIR temperature.....	57
Figure 30 Input and output species of the SIR applied in carbon monoxide to hydrogen conversion.....	58
Figure 31 Hydrogen production with carbon monoxide as SIR reducing agent .....	58
Figure 32 Carbon monoxide utilisation as a function of SIR operating temperature .....	59

## List of tables

Table 1 Composition of inlet gas, lean gas and product hydrogen after conversion in the SIR .....	10
Table 2 Composition of the Martian atmosphere.....	13
Table 3 Elemental composition of samples at the Viking 1 Lander and MPF Lander sites..	14
Table 4 Mineralogy of samples at the Viking 1 Lander and MPF Lander sites .....	14
Table 5 Comparison of mineralogy .....	17
Table 6 Overview of potential RESC input species covered within the initial investigations	28
Table 7 Bulk data of RESC input species investigated .....	29
Table 8 RESC simulation parameters, reference case .....	29
Table 9 Overview of the molar flux of species within the reduction cycle of the RESC per mole of methane fuel supplied .....	30
Table 10 Overview of the molar flux of species within the reduction cycle of the RESC per mole of heptane fuel supplied .....	30
Table 11 Overview of temperatures and thermal energy balance for the reduction cycle of the RESC .....	31
Table 12 Overview of process temperatures and thermal energy balance for the oxidation cycle of the RESC .....	32
Table 13 Compressed mass balance for the investigated input gases .....	36
Table 14 Gravimetric and volumetric transport efficiency for investigated input species .....	37
Table 15 Oxygen requirement for lean gas burner and input oxygen/fuel input gas streams for external burner unit .....	37
Table 16 Oxygen requirement per mole of hydrogen produced .....	38
Table 17 Compressed thermal energy balance for the investigated input gases.....	38
Table 18 Maximum conversion efficiencies computed for the RESC with different input species .....	42
Table 19 Results of the RESC input species evaluation process.....	43
Table 20 Energy balance of the fuel cell module .....	46
Table 21 Overview of hydrocarbon fuel to electric conversion efficiencies for the seven investigated RESC input species .....	47
Table 22 Energy balance for the RESC reduction cycle .....	50
Table 23 Energy balance for the RESC oxidation cycle.....	51
Table 24 Energy balance for the fuel cell unit .....	52
Table 25 Energy balance for the hydrocarbon to electric conversion process .....	52
Table 26 Theoretical hydrogen storage capacity as a function of final iron oxide stage .....	60
Table 27 Chemical composition of Lunar soils .....	69

Table 28 Evaluation scores derived with the input species transport and storage properties .....	70
Table 29 Evaluation scores derived with the RESC system dimensions properties .....	70
Table 30 Evaluation scores derived with hydrocarbon to hydrogen conversion efficiencies	71

## References

---

- 1 A. Messerschmitt, Verfahren zur Erzeugung von Wasserstoff durch abwechselnde Oxidation und Reduktion von Eisen in von außen beheizten, in den Heizräumen angeordneten Zersetzern, DE 266863, Germany, 1911.
- 2 V. Hacker, R. Fankhauser, G. Faleschini, H. Fuchs, K. Friedrich, M. Muhr, K. Kordes, Hydrogen production by steam iron process, *J. Power Sources*, 86 (1–2) (2000) 531–535.
- 3 V. Hacker, G. Faleschini, H. Fuchs, R. Fankhauser, G. Simader, M. Ghaemi, B. Spreitz, K. Friedrich, Usage of biomass gas for fuel cells by SIR process, *J. Power Sources*, 71 (1998) 226-230.
- 4 V. Hacker, A novel process for stationary hydrogen production: The Reformer Sponge Iron Cycle (RESC), *J. Power Sources*, 118 (2003) 311–314.
- 5 M. Thaler, V. Hacker, A. Mettu, J.O. Besenhard, et al., Investigations of cycle behaviour of the contact mass in the RESC process for hydrogen production, *International Journal of Hydrogen Energy*, 2004, submitted.
- 6 K.K. Bhatia, C.-Y. Wang, Transient carbon monoxide poisoning of a polymer electrolyte fuel cell operating on diluted hydrogen feed, *Electrochimica Acta*, 49 (2004) 2333–2341.
- 7 J. Divisek, H.-F. Oetjen, V. Peinecke, V.M. Schmidt, U. Stimming, Components for PEM fuel cell systems using hydrogen and CO containing fuels, *Electrochimica Acta*, 43 (1998) 3811-3815.
- 8 V. Hacker, H. Fuchs, Sponge iron reactor (SIR) for energy storage and gas conditioning, Final Report of Project P13030-TEC.
- 9 D.R. Williams, NASA Moon fact sheet, <http://nssdc.gsfc.nasa.gov/planetary/factsheet/moonfact.html>, 02/2005.
- 10 NASA JSC, Mining and manufacturing on moon, <http://aerospacescholars.jsc.nasa.gov/HAS/cirr/em/8/4.cfm>, 02/2005.
- 11 C. Allen, Lunar oxygen – ground truth and predictions, <http://ares.jsc.nasa.gov/HumanExplore/Exploration/EXLibrary/docs/BeyondLEO/leo195/lunox.htm>, 02/2005.
- 12 D.R. Williams, Clementine project information, <http://nssdc.gsfc.nasa.gov/planetary/clementine.html>, 02/2005.

---

13 J.J. Gillis, B.J. Jolliff, R.L. Korotev, Lunar surface geochemistry: Global concentrations of Th, K, and FeO as derived from lunar prospector and Clementine data, *Geochimica et Cosmochimica Acta*, Vol. 68, No. 18, pp. 3791–3805, 2004.

14 K. Joosten, The air up there – lunar resources and the economics of exploration, <http://ares.jsc.nasa.gov/HumanExplore/Exploration/EXLibrary/docs/BeyondLEO/leo394/air.htm>, 02/2005.

15 NASA/JSC image #S93-45590, <http://ares.jsc.nasa.gov/HumanExplore/Exploration/EXLibrary/images/Pics/LUNOX/02ISRU.gif>, 02/2005.

16 D.R. Williams, NASA Mars fact sheet, <http://nssdc.gsfc.nasa.gov/planetary/factsheet/marsfact.html>, 02/2005.

17 T.R. Meyer, C.P. McKay, Using the resources of Mars for human settlement, AAS books on Mars exploration, Volume 86, AAS Science and Technology Series, Univelt, 1996.

18 NASA NSSDC, Preliminary Mars Pathfinder APSX results, [http://nssdc.gsfc.nasa.gov/planetary/marspath/apxs\\_table1.html](http://nssdc.gsfc.nasa.gov/planetary/marspath/apxs_table1.html), 02/2005.

19 R. Rieder, T. Economou, H. Wänke, A. Turkevich, J. Crisp, et al., The chemical composition of Martian soil and rocks returned by the Mobile Alpha Proton X-ray Spectrometer: preliminary results from the X-ray mode, *Science*, Vol 278, Issue 5344, 1771-1774, 1997.

20 H.Y. McSween, K. Keil, Mixing relationships in the Martian regolith and the composition of globally homogeneous dust, *Geochimica et Cosmochimica Acta*, 64, 12, pp. 2155-2166, 2000.

21 Cornell University, Athena science package home page, <http://athena.cornell.edu/>, 02/2005.

22 Cornell University, Instruments - Mini-Thermal Emission Spectrometer, [http://athena.cornell.edu/the\\_mission/ins\\_minites.html](http://athena.cornell.edu/the_mission/ins_minites.html), 02/2005.

23 Cornell University, Instruments - Mössbauer Spectrometer, [http://athena.cornell.edu/the\\_mission/ins\\_moss.html](http://athena.cornell.edu/the_mission/ins_moss.html), 02/2005.

24 Hoffman, S.J. (ed.), Kaplan, D.I. (ed.), The Reference Mission of the NASA Mars Exploration Study Team, NASA Human Mission Study Lead, Exploration Office.

25 G.J. Taylor (ed.), P.D. Spudis (ed.), Geoscience and a lunar base, A comprehensive plan for lunar exploration, NASA Conference Publication 3070.

- 
- 26 J.R. Rostrup-Nielsen, Catalytic steam reforming, in: J.R. Anderson and M. Boudart (Eds.), *Catalysis – Science and Technology*, Springer, Vol. 5, 1984.
- 27 J.R. Rostrup-Nielsen, New aspects of syngas production and use, *Catalysis Today*, 63 (2000) 159 – 164.
- 28 J.R. Rostrup-Nielsen, K. Aasberg-Petersen, in: W. Vielstich, H.A. Gasteiger, A. Lamm (Eds.), *Handbook of Fuel Cells – Fundamentals, Technology and Applications*, Vol. 3, John Wiley & Sons, 2003, pp. 159-176.
- 29 J.R. Rostrup-Nielsen, Industrial relevance of coking, *Catalysis Today*, 37 (1997) 225-232.
- 30 I. Barin, D. Neuschütz, Calculation of the equilibrium compositions and soot formation boundaries in the system C-CH<sub>4</sub>-H<sub>2</sub>-CO-H<sub>2</sub>O-CO<sub>2</sub>, *Arch. Eisenhüttenwesen*, 46 (1975) 159-164.
- 31 T.S. Christensen, Adiabatic prereforming of hydrocarbons – an important step in syngas production, *Applied Catalysis A: General*, 138 (1996) 285-309.
- 32 S. Gordon, B.J. McBride, *Computer Program for Calculation of Complex Chemical Equilibrium Compositions and Applications*, NASA Reference Publication 1311, 1994.
- 33 I. Barin, *Thermochemical Data of Pure Substances*, VCH Weinheim, 1989.
- 34 E. Achenbach, Three dimensional and time-dependant simulation of a planar solid oxide fuel cell, *Journal of Power Sources*, Vol. 49, pp. 333 – 348, 1994



## Appendix A: Chemical composition of Lunar soils

**Table 30** Chemical compositions (wt.%) of average soils at lunar landing sites and in selected regions at the Apollo 15, Apollo 16, Apollo 17, Luna 16, Luna 20, and Luna 24 sites<sup>1</sup>

	11	12	14	15a	15b	15c	15	16a	16b	16c	16	17a	17b	17c	17d	17	L16	L20	L24
SiO <sub>2</sub>	42.2	46.3	48.1	46.7	46.6	47.1	46.8	45.0	44.9	45.1	45.0	40.6	45.1	43.5	43.7	43.2	41.7	45.1	43.9
TiO <sub>2</sub>	7.8	3.0	1.7	1.7	1.4	1.0	1.4	0.56	0.47	0.60	0.54	8.4	1.7	3.4	3.5	4.2	3.4	0.55	1.3
Al <sub>2</sub> O <sub>3</sub>	13.6	12.9	17.4	13.2	17.1	13.4	14.6	27.1	28.0	26.8	27.3	12.0	20.7	18.0	17.4	17.1	15.3	22.3	12.5
Cr <sub>2</sub> O <sub>3</sub>	0.30	0.34	0.23	0.44	0.27	0.37	0.36	0.34	0.54	0.11	0.33	0.45	0.25	0.28	0.32	0.33	0.28		0.32
FeO <sup>2-</sup>	15.3	15.1	10.4	16.3	11.7	14.9	14.3	5.2	4.7	5.4	5.1	16.7	8.8	10.9	12.2	12.2	16.7	7.0	19.8
MnO	0.20	0.22	0.14	0.21	0.16	0.19	0.19	0.41	0.27	0.22	0.30	0.23	0.12	0.16	0.16	0.17	0.23	0.13	0.25
MgO	7.8	9.3	9.4	10.9	10.5	13.0	11.5	5.8	5.6	5.7	5.7	9.9	9.8	10.7	11.1	10.4	8.8	9.8	9.4
CaO	11.9	10.7	10.7	10.4	11.6	10.3	10.8	15.8	15.7	15.6	15.7	10.9	12.8	12.12	11.3	11.8	12.5	15.1	12.3
Na <sub>2</sub> O	0.47	0.54	0.70	0.38	0.45	0.33	0.39	0.46	0.50	0.43	0.46	0.35	0.42	0.42	0.42	0.40	0.34	0.50	0.31
K <sub>2</sub> O	0.16	0.31	0.55	0.23	0.20	0.19	0.21	0.13	0.23	0.14	0.17	0.16	0.16	0.12	0.09	0.13	0.10	0.10	0.04
P <sub>2</sub> O	0.05	0.4	0.51	0.16	0.19	0.19	0.18	0.13	0.10	0.10	0.11	0.14	0.15	0.09	0.08	0.12	0.12	0.16	0.11
S	0.12			0.07	0.08	0.04	0.06	0.07	0.05	0.09	0.07	0.12	0.09	0.07	0.09	0.09	0.21	0.08	0.14
Total	99.9	99.6	99.8	100.6	100.2	100.9	100.8	100.9	100.9	100.4	100.8	100.1	100.0	99.8	99.9	100.5	99.7	100.8	100.4

- 11 Composition of soil 10002 from Apollo 11 site.
- 12 Average composition of selected soils (12001, 12023, 12030, 12032, 12033, 12037, 12041, 12042, 12044, 12070) from the Apollo 12 site.
- 14 Average composition of selected soils (14003, 14148, 14149, 14156) from the Apollo 14 site.
- 15a Average composition of selected mare soils (15012, 15013, 15020, 15030, 15040, 15070, 15080, 15470, 15500, 15530, 15600) from the Apollo 15 site.
- 15b Average composition of selected Apennine Front soils (15090, 15100, 15210, 15221, 15230, 15250, 15270, 15290) from the Apollo 15 site.
- 15c Average composition of selected green-glass-rich soils (15300, 15400, 15410, 15403) from the Apollo 15 site.
- 15 Average composition of Apollo 15 soils.
- 16a Average composition of Cayley Plain soil (60050, 60500, 61140, 61161, 61180, 61220, 61240, 61500, 62240, 62280) from the Apollo 16 site.
- 16b Average composition of selected North Ray soils (63320, 63340, 63500, 67460, 67480, 67600, 67700, 67710, 68500, 68820, 69920, 69940) from the Apollo 16 site.
- 16c Average composition of selected Stone Mountain and South Ray soils (64420, 64500, 64800, 65500, 65700, 66040, 66080) from the Apollo 16 site.
- 16 Average composition of Apollo 16 soils.
- 17a Average composition of selected mare soils (70011, 70160, 70180, 71040, 71060, 71500, 72160, 75060, 75080, 79220, 79240) from the Apollo 17 site.
- 17b Average composition of selected South Massif and light mantle soils (72320, 72440, 72460, 72500, 73120, 73140, 73220, 73280, 74120) from the Apollo 17 site.
- 17c Average composition of selected North Massif soils (76246, 76260, 76280, 76320, 76500, 77530) from the Apollo 17 site.
- 17d Average composition of selected Sculptured Hill soils (78220, 78420, 78440, 78460, 78480) from the Apollo 17 site.
- 17 Average composition of Apollo 17 soils.
- L16 Average composition of Luna 16 soils (Russian data).
- L20 Average composition of Luna 20 soils (Russian data).
- L24 Average composition of Luna 24 soils (Russian data).

<sup>1</sup> adapted from USGS Astrogeology Research Program,  
[http://astrogeology.usgs.gov/Projects/LunarConsortium/data/chem\\_min/tab7\\_15.doc](http://astrogeology.usgs.gov/Projects/LunarConsortium/data/chem_min/tab7_15.doc), 02/2005

## Appendix B: Evaluation score tables

**Table 28** Evaluation scores derived with the input species transport and storage properties

	Density <sup>1</sup>	Boiling temperature <sup>1</sup>	Score	Gravimetric energy density <sup>2</sup>	Score	Volumetric energy density	Score	Overall score
	kg/m <sup>3</sup>	°C	-	MJ/kg	-	MJ/liter	-	-
Methane (liquid)	423	-161.6	7	50	1	21	5	13
Propane (liquid)	582	-42.1	6	46	2	27	3	11
Butane (liquid)	601	-0.5	5	46	2	27	3	10
Heptane	680	98.0	2	44	5	30	2	9
Octane	700	126.0	1	45	4	31	1	6
Methanol	790	64.5	4	20	7	16	7	18
Ethanol	790	78.0	3	27	6	21	5	14

<sup>1</sup>Derived from MSDS, airliquide, <http://www.us.airliquide.com/en/business/msds/category/pure.asp>

<sup>2</sup>Derived from W.Beitz, K.-H. Grote, Dubbel, 19th ed., Springer, 1997

**Table 29** Evaluation scores derived with the RESC system dimensions properties

	Internal flow rate	Score	Reduction cycle heat recuperation system size	Score	Thermal energy input	Score	Lean gas burner oxygen consumption	Score	Total score
	mole/mole <sub>H2</sub>	-	kJ/mole <sub>H2</sub>	-	kJ/mole <sub>H2</sub>	-	mole/mole <sub>H2</sub>	-	-
<b>Methane</b>	2.2	5	137.6	5	30.5	5	0.2	5	<b>20</b>
<b>Propane</b>	2.0	4	128.6	4	12.1	3	0.2	4	<b>15</b>
<b>Butane</b>	1.9	3	127.6	3	13.1	4	0.2	3	<b>13</b>
<b>Heptane</b>	1.9	2	126.4	2	34.1	7	0.2	2	<b>13</b>
<b>Octane</b>	1.9	1	126.2	1	34.1	6	0.2	1	<b>9</b>
<b>Methanol</b>	3.4	7	210.4	7	0.0	1	0.3	7	<b>22</b>
<b>Ethanol</b>	2.5	6	160.2	6	10.7	2	0.3	6	<b>20</b>

**Table 30** Evaluation scores derived with the hydrocarbon to hydrogen conversion efficiency criteria

	Efficiency with external burner	Score	Efficiency without external burner	Score
	%	-	%	-
<b>Methane</b>	74.8	6	84.0	5
<b>Propane</b>	79.8	1	84.9	4
<b>Butane</b>	79.7	2	85.3	3
<b>Heptane</b>	75.0	4	86.4	2
<b>Octane</b>	75.0	3	86.5	1
<b>Methanol</b>	67.6	7	67.6	7
<b>Ethanol</b>	74.8	5	77.9	6